US 20060000803A1

(19) United States

(12) Patent Application Publication (10) Pub. No.: US 2006/0000803 A1

Koshiishi et al. (43) Pub. Date: Jan. 5, 2006

(54) PLASMA PROCESSING METHOD AND APPARATUS

(76) Inventors: **Akira Koshiishi**, Nirasaki-shi (JP); **Jun Hirose**, Nirasaki-shi (JP); **Masahiro Ogasawara**, Nirasaki-shi (JP); **Taichi Hirano**, Nirasaki-shi (JP); **Hiromitsu Sasaki**, Kurihara-gun (JP); **Tetsuo Yoshida**, Nirasaki-shi (JP); **Michishige Saito**, Nirasaki-shi (JP); **Hiroyuki Ishihara**, Nirasaki-shi (JP); **Jun Ooyabu**, Nirasaki-shi (JP); **Kohji Numata**, Kyoto-shi (JP)

Correspondence Address:
OBLON, SPIVAK, MCCLELLAND, MAIER & NEUSTADT, P.C.
1940 DUKE STREET
ALEXANDRIA, VA 22314 (US)

(21) Appl. No.: **11/137,673**

(22) Filed: **May 26, 2005**

Related U.S. Application Data

(63) Continuation of application No. PCT/JP03/15029, filed on Nov. 25, 2003.

(30) **Foreign Application Priority Data**

Nov. 26, 2002 (JP) 2002-341949
Oct. 17, 2003 (JP) 2003-358432

Publication Classification

(51) **Int. Cl.**
C23F 1/00 (2006.01)

(52) **U.S. Cl.** **216/67**; 156/345.47

(57) **ABSTRACT**

A plasma processing method is arranged to supply a predetermined process gas into a plasma generation space in which a target substrate is placed, and turn the process gas into plasma. The substrate is subjected to a predetermined plasma process by this plasma. The spatial distribution of density of the plasma and the spatial distribution of density of radicals in the plasma are controlled independently of each other relative to the substrate by a facing portion opposite the substrate to form a predetermined process state over the entire target surface of the substrate.

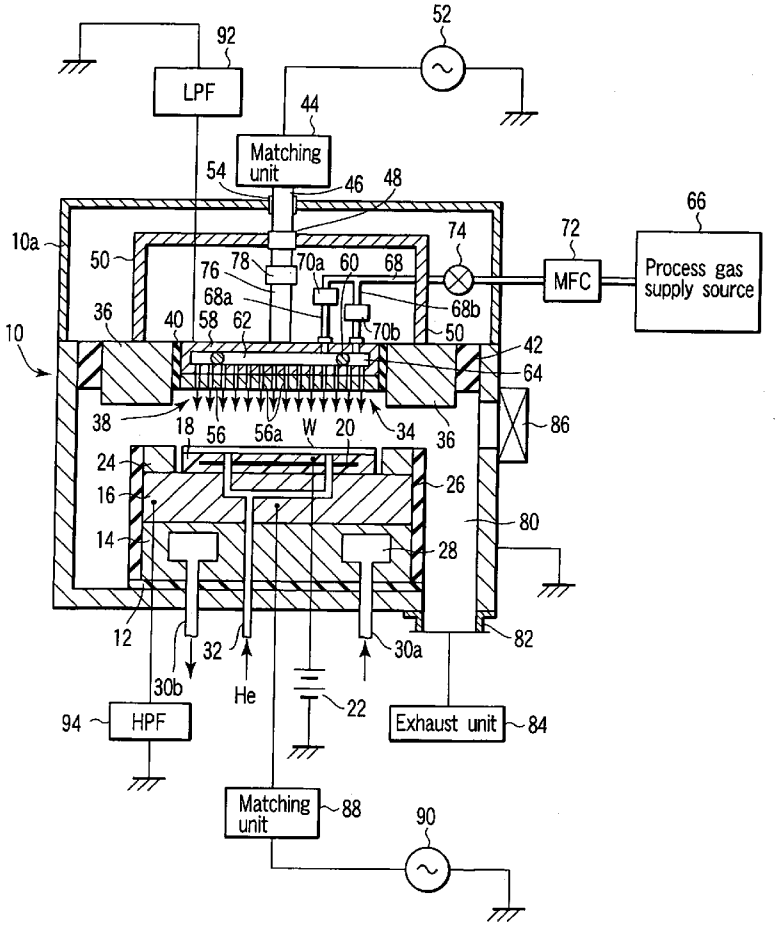

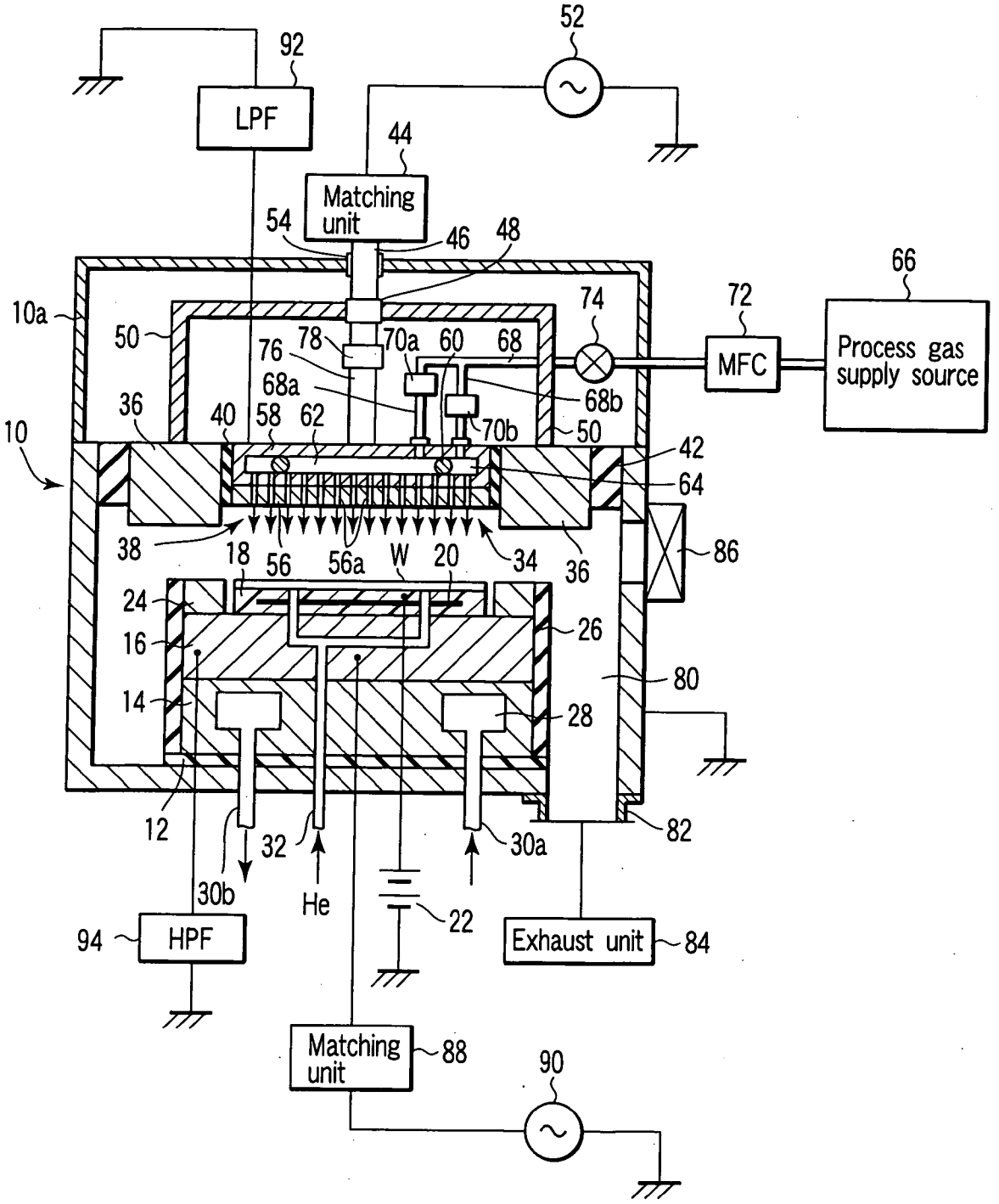
52
92
LPF
44
Matching unit
54
46
48
66
74
72
10a
50
76
78
70a
60
68
MFC
Process gas supply source
68a
68b
36
40
58
62
70b
50
10
42
64
38
18
56
56a
W
20
34
36
86
24
26
16
80
14
28
12
32
30a
82
30b
He
22
94
HPF
Exhaust unit
84
Matching unit
88
90

FIG. 1

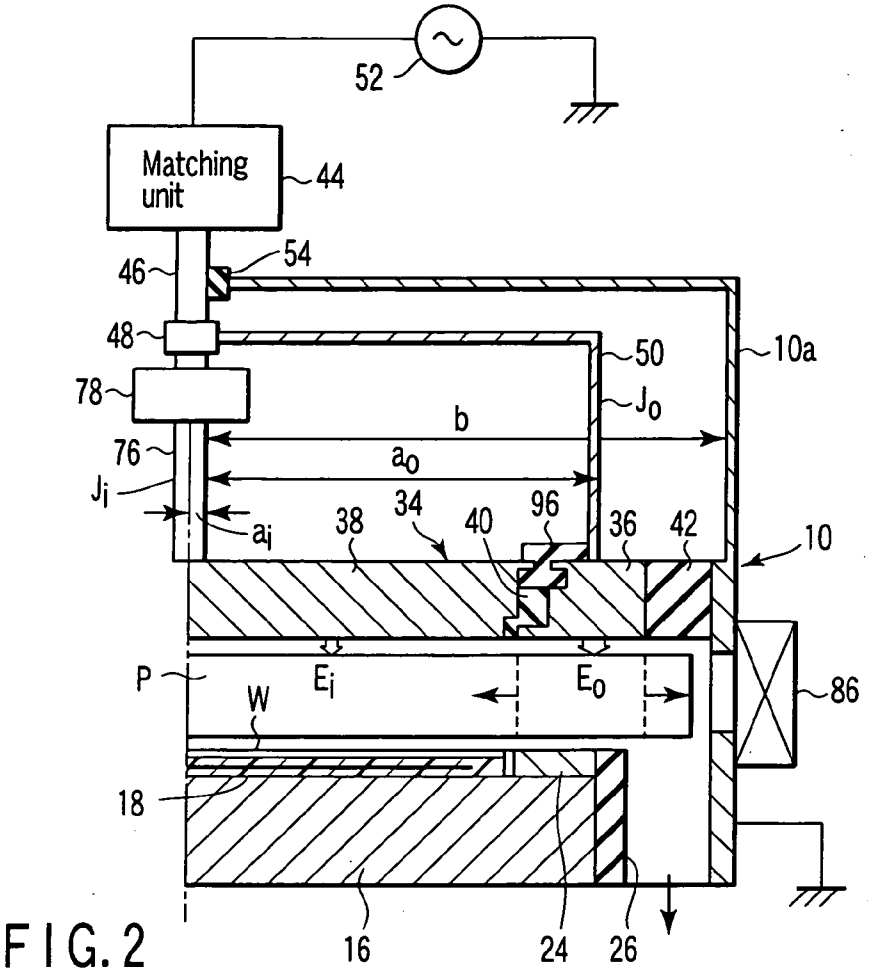
52
Matching unit
44
46
54
48
50
10a
78
J_o
b
76
a_o
J_i
a_i
38
34
40
96
36
42
10
P
E_i
E_o
86
W
18
16
24
26

FIG. 2

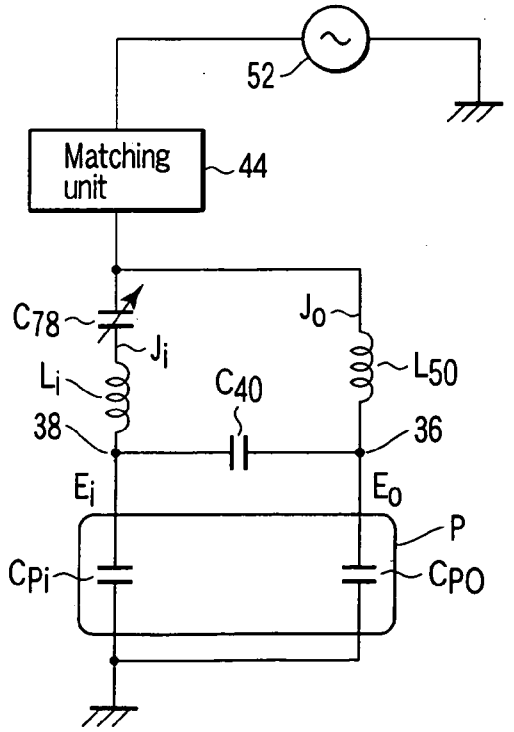
52
Matching unit
44
C_{78}
J_i
J_o
L_i
C_{40}
L_{50}
38
36
E_i
E_o
P
C_{Pi}
C_{PO}

FIG. 3

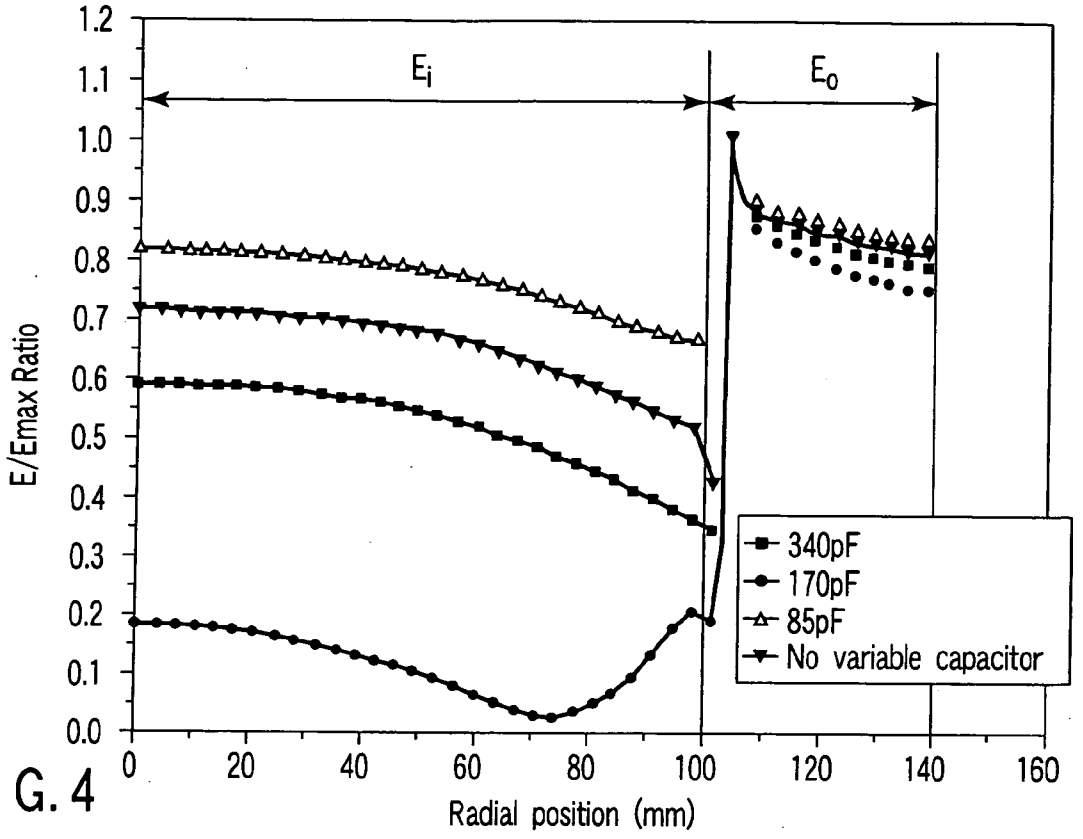
E/Emax Ratio
Radial position (mm)
E_i
E_o
340pF
170pF
85pF
No variable capacitor
1.2
1.1
1.0
0.9
0.8
0.7
0.6
0.5
0.4
0.3
0.2
0.1
0.0
0
20
40
60
80
100
120
140
160

FIG. 4

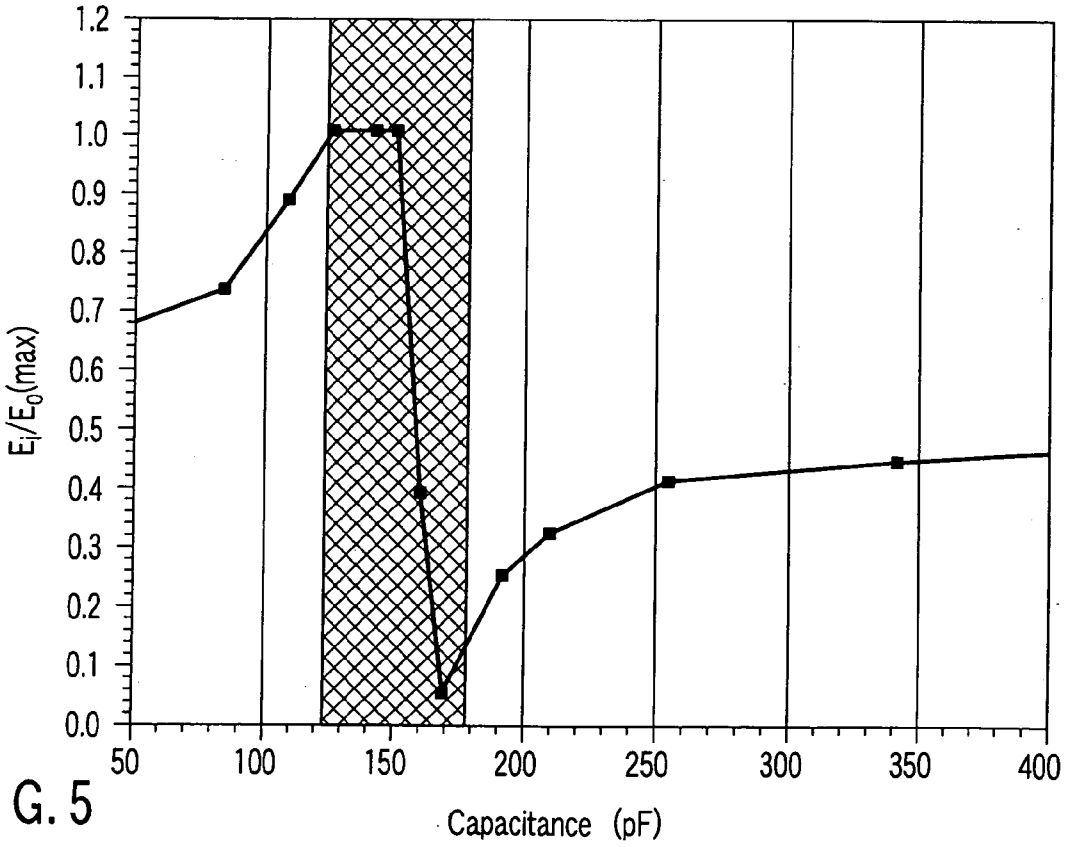
E_i/E_0(max)
Capacitance (pF)
1.2
1.1
1.0
0.9
0.8
0.7
0.6
0.5
0.4
0.3
0.2
0.1
0.0
50
100
150
200
250
300
350
400

FIG. 5

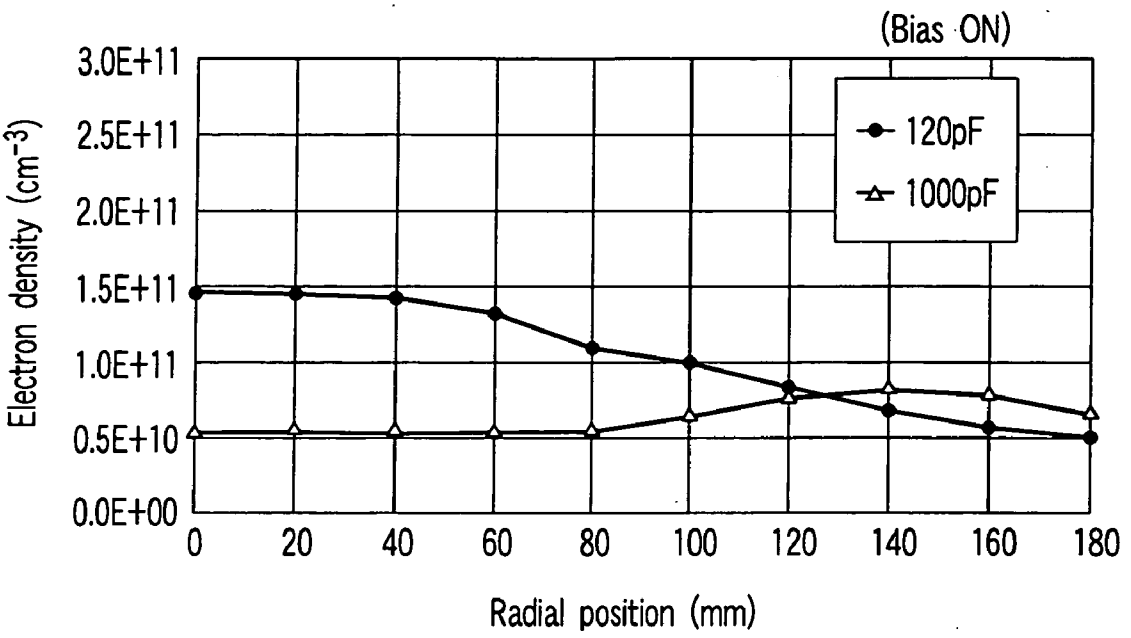
(Bias ON)
3.0E+11
2.5E+11
2.0E+11
1.5E+11
1.0E+11
0.5E+10
0.0E+00
Electron density (cm-3)
120pF
1000pF
0
20
40
60
80
100
120
140
160
180
Radial position (mm)

FIG. 6A

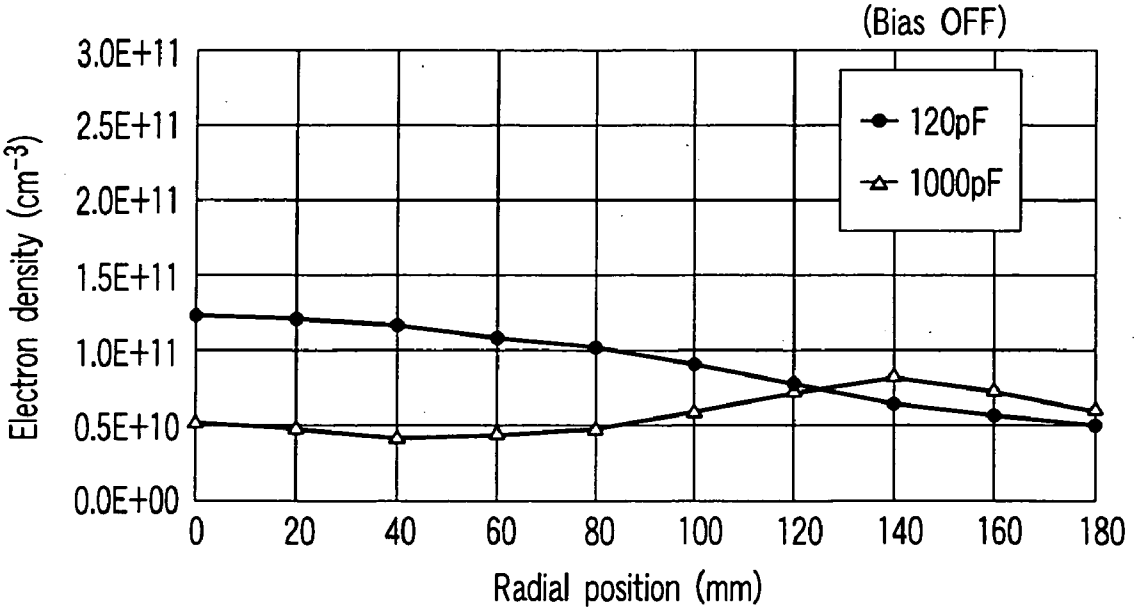
(Bias OFF)
3.0E+11
2.5E+11
2.0E+11
1.5E+11
1.0E+11
0.5E+10
0.0E+00
Electron density (cm-3)
120pF
1000pF
0
20
40
60
80
100
120
140
160
180
Radial position (mm)

FIG. 6B

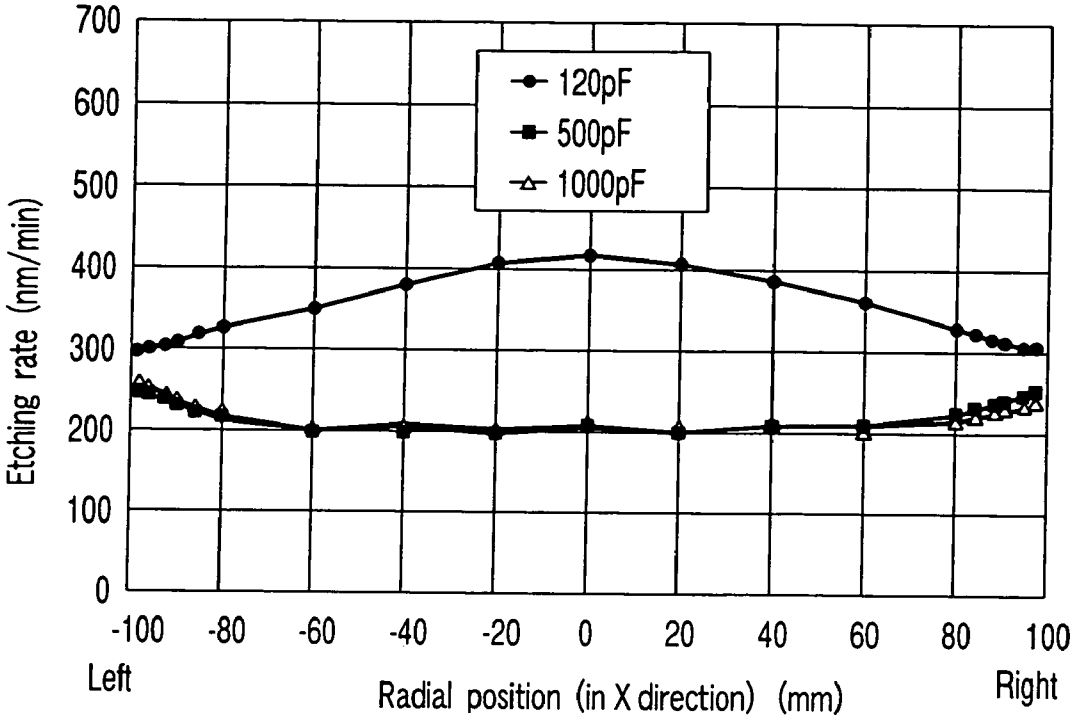
700
600
500
400
300
200
100
0
Etching rate (nm/min)
120pF
500pF
1000pF
-100
-80
-60
-40
-20
0
20
40
60
80
100
Left
Radial position (in X direction) (mm)
Right

FIG. 7A

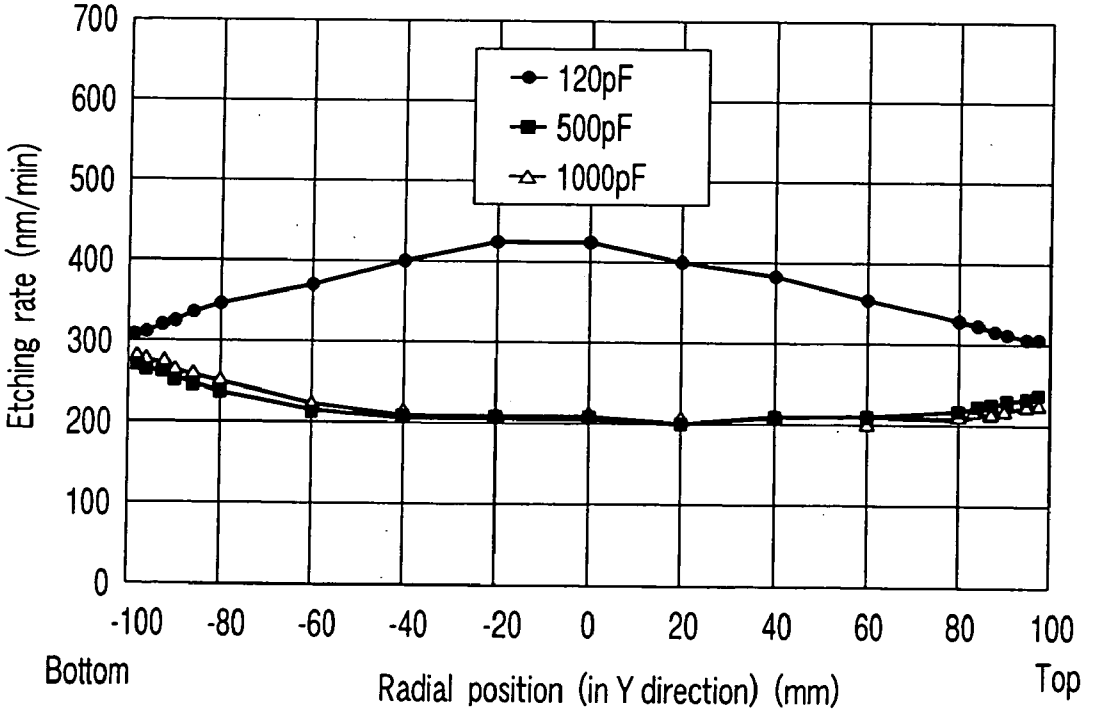
700
600
500
400
300
200
100
0
Etching rate (nm/min)
120pF
500pF
1000pF
-100
-80
-60
-40
-20
0
20
40
60
80
100
Bottom
Radial position (in Y direction) (mm)
Top

FIG. 7B

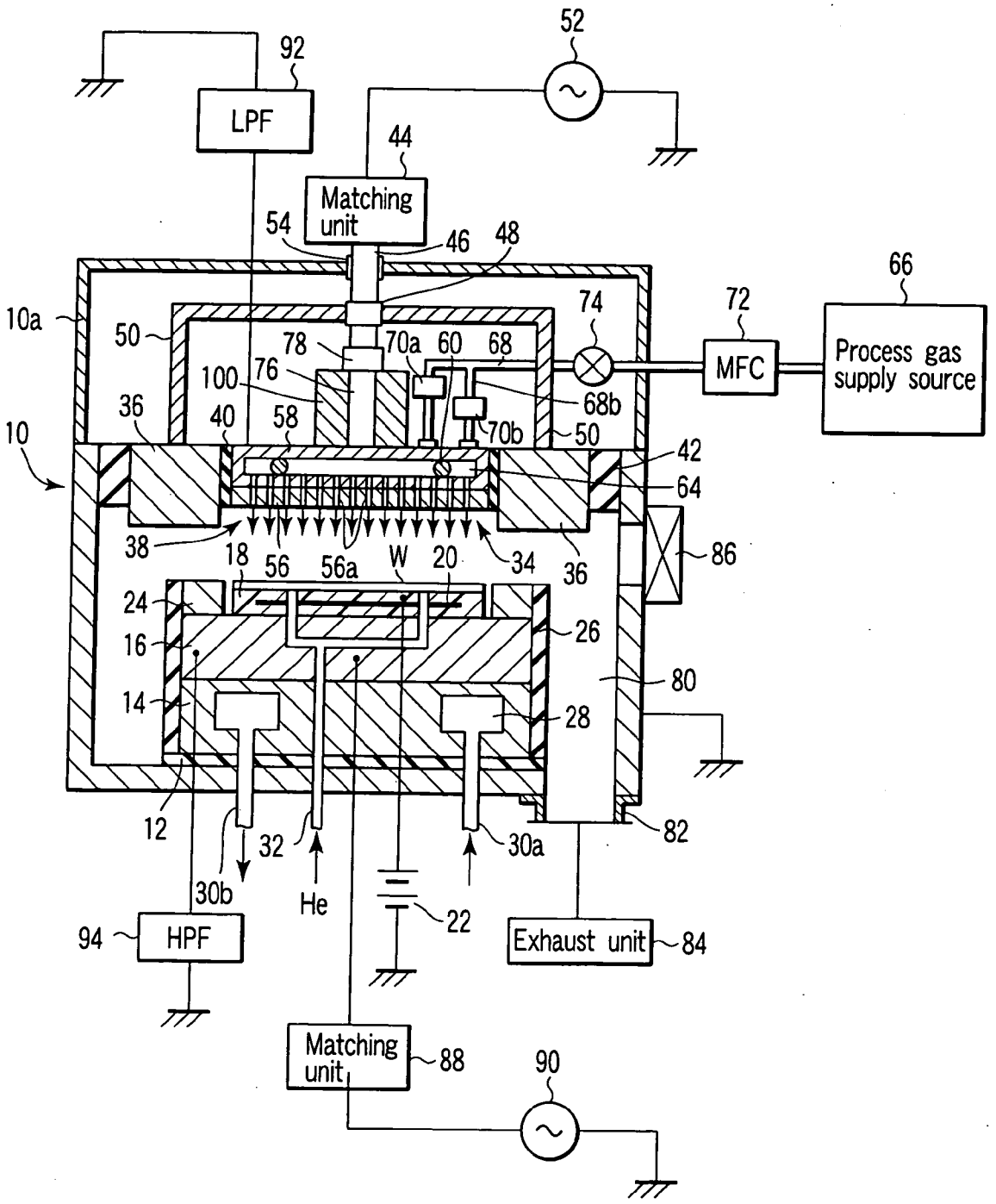
52
92
LPF
44
Matching unit
54
46
48
66
74
72
10a
50
78
70a
60
68
MFC
Process gas supply source
100
76
68b
36
40
58
70b
50
10
42
64
38
18
56
56a
W
20
34
36
86
24
26
16
80
14
28
12
32
30a
82
30b
He
22
94
HPF
Exhaust unit
84
Matching unit
88
90

FIG. 8

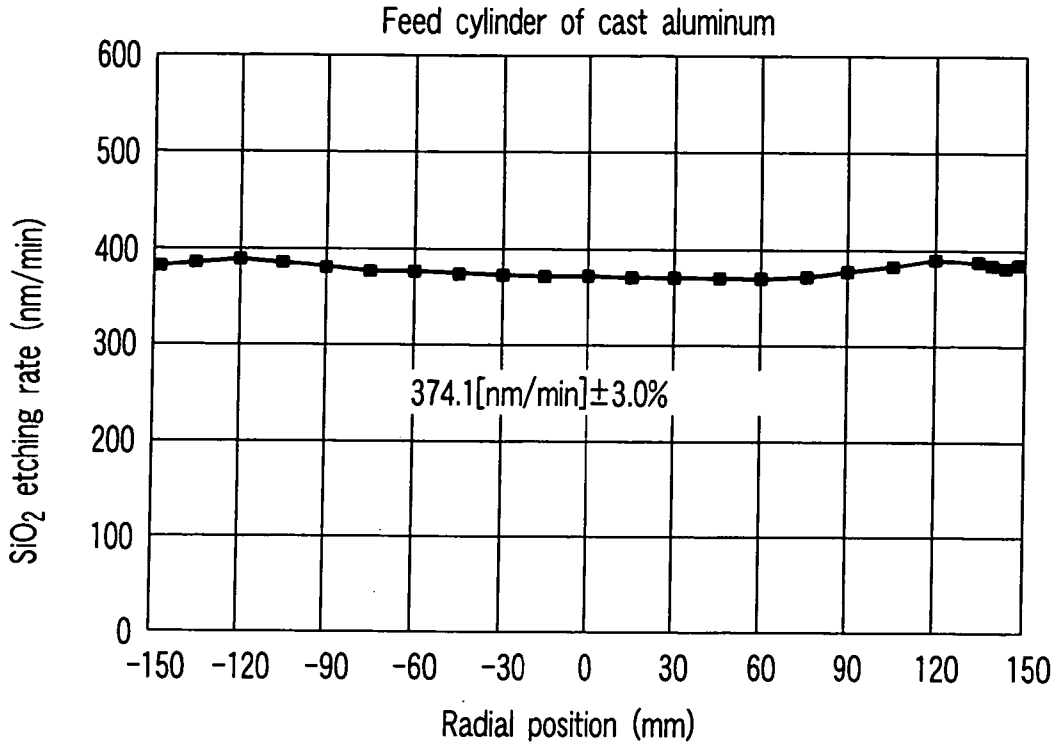
Feed cylinder of cast aluminum
600
500
400
300
200
100
0
SiO_2 etching rate (nm/min)
374.1[nm/min]±3.0%
-150 -120 -90 -60 -30 0 30 60 90 120 150
Radial position (mm)

FIG. 9A

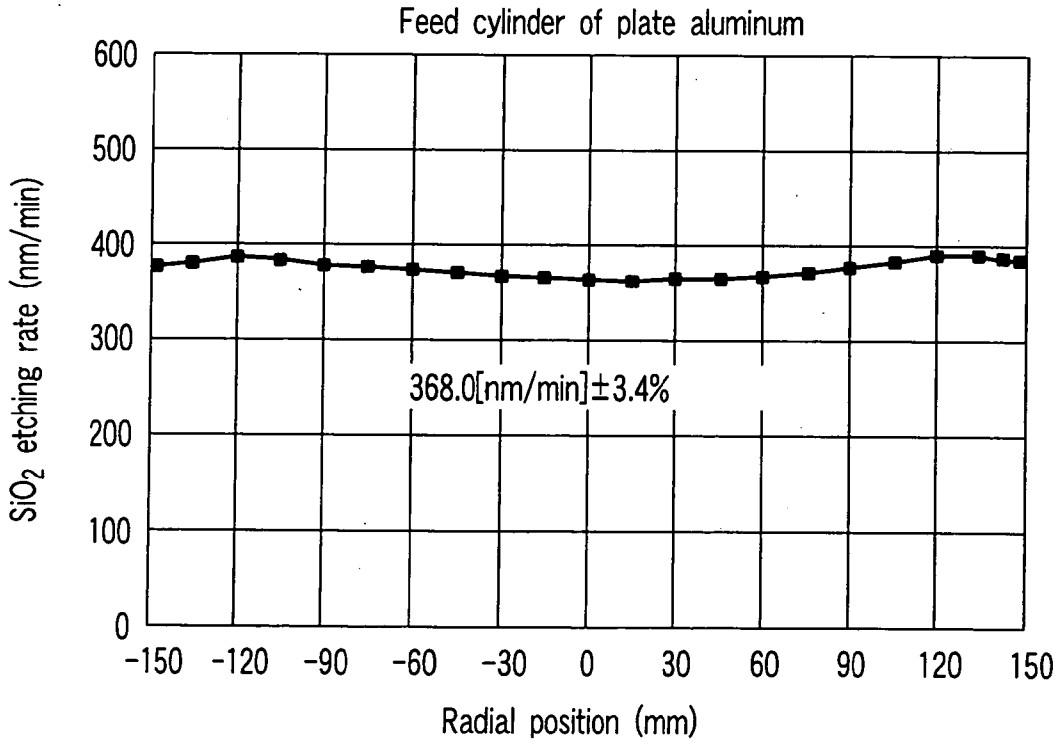
Feed cylinder of plate aluminum
600
500
400
300
200
100
0
SiO_2 etching rate (nm/min)
368.0[nm/min]±3.4%
-150 -120 -90 -60 -30 0 30 60 90 120 150
Radial position (mm)

FIG. 9B

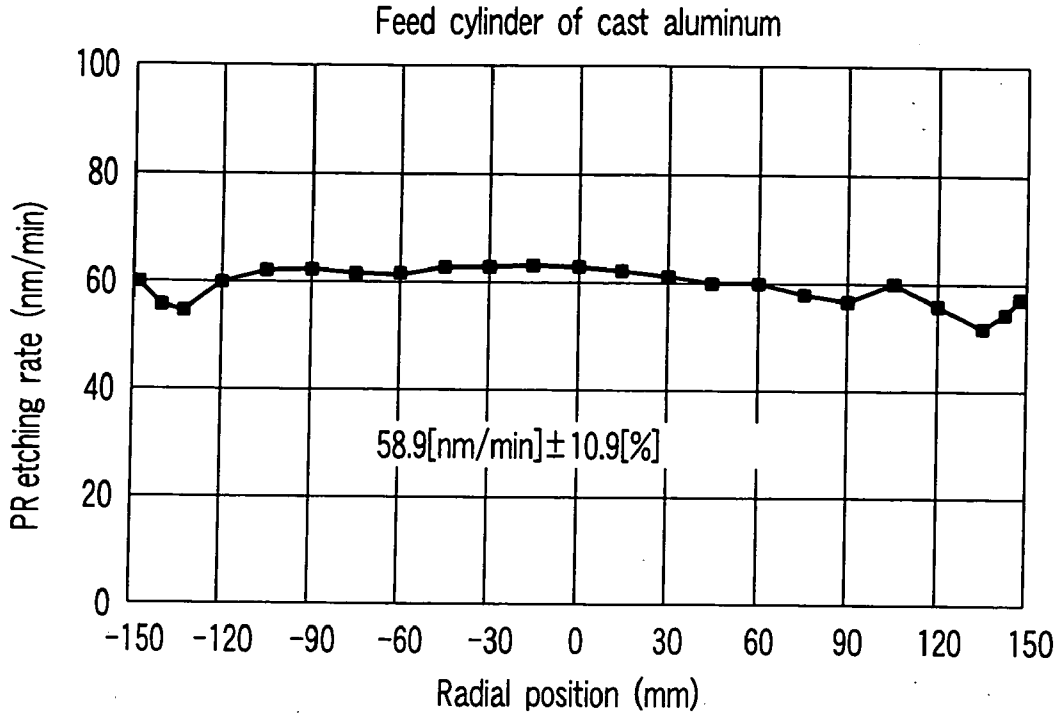

FIG. 10A

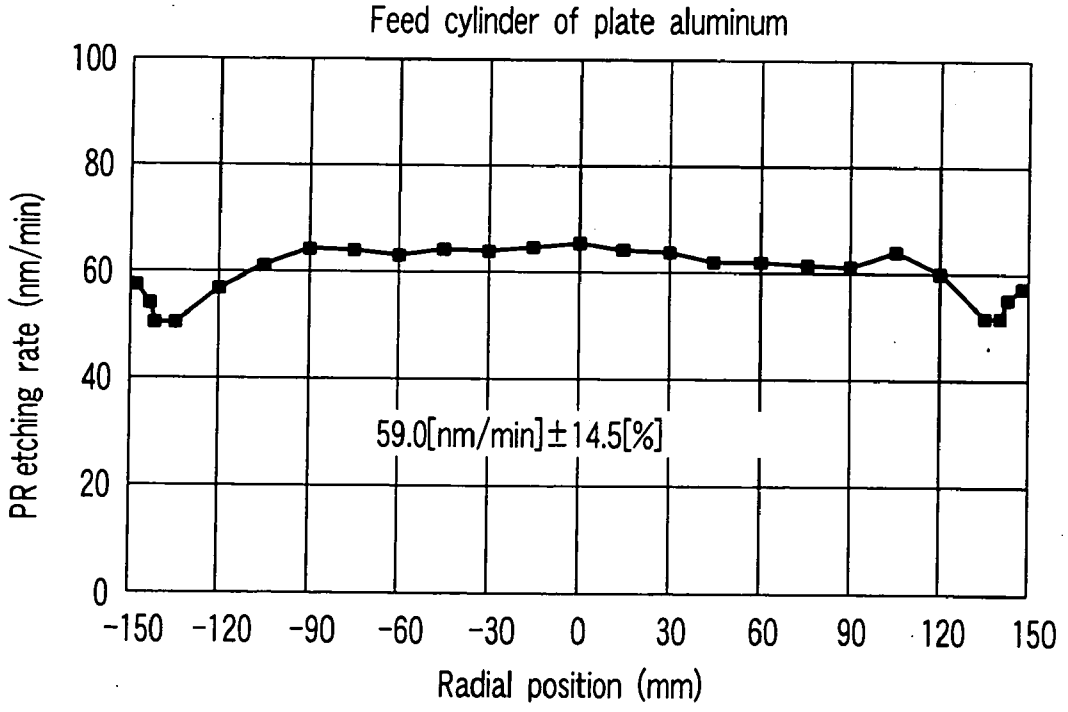

FIG. 10B

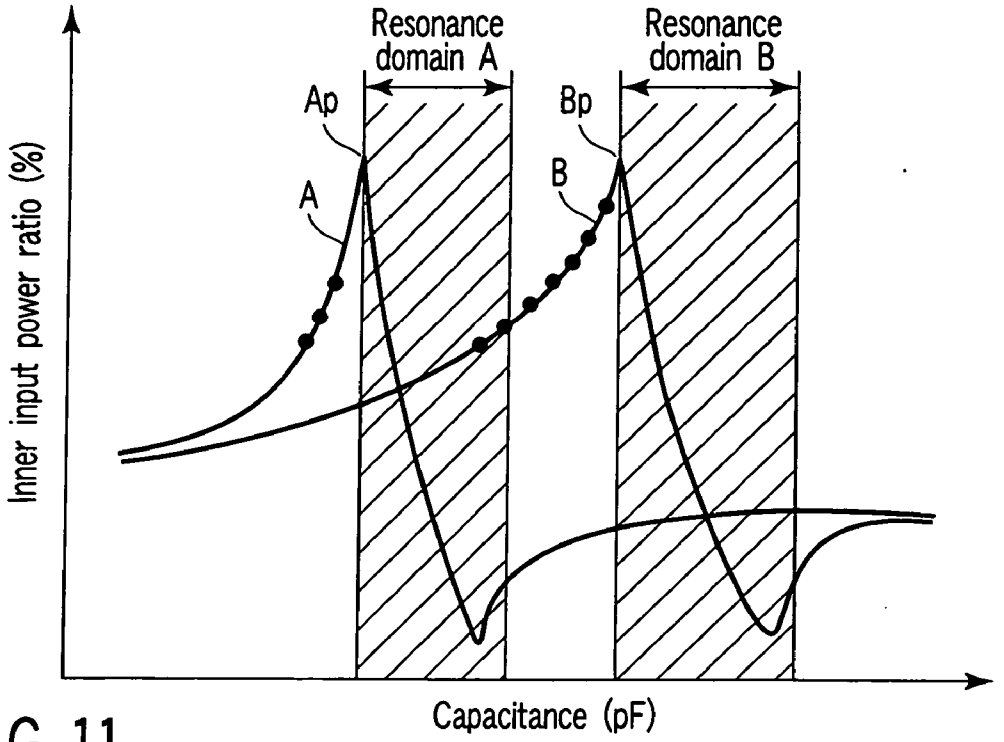
Resonance domain A
Resonance domain B
Ap
Bp
A
B
Inner input power ratio (%)
Capacitance (pF)

FIG. 11

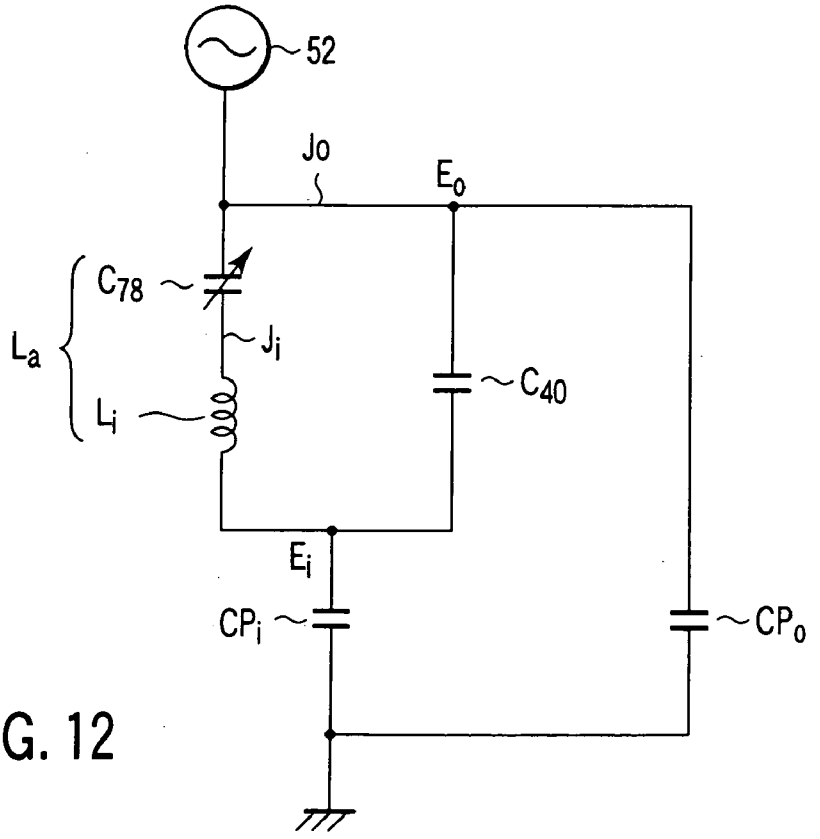
52
Jo
E_o
C_{78}
J_i
L_a
L_i
C_{40}
E_i
CP_i
CP_o

FIG. 12

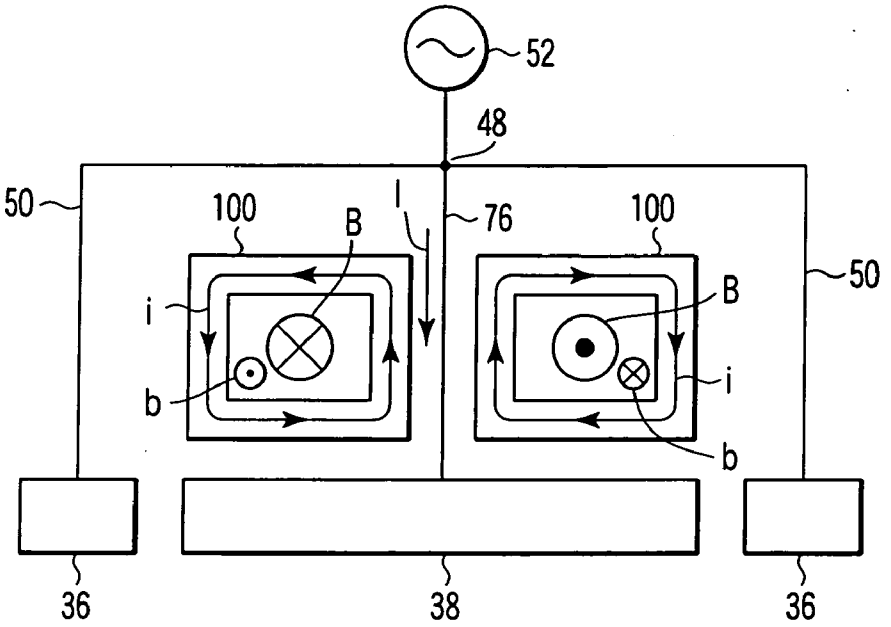
52
48
50
100
B
I
76
100
50
i
B
i
b
b
36
38
36

FIG. 13

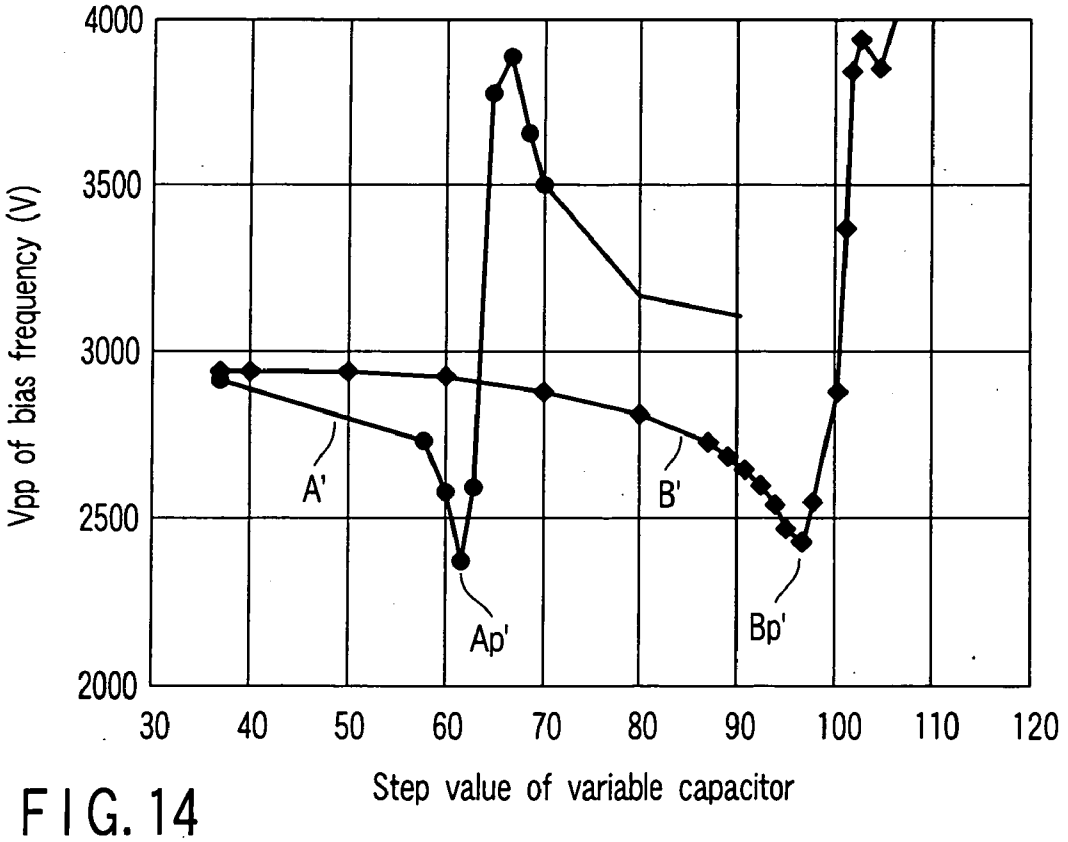
4000
3500
3000
2500
2000
Vpp of bias frequency (V)
30
40
50
60
70
80
90
100
110
120
Step value of variable capacitor
A'
B'
Ap'
Bp'

FIG. 14

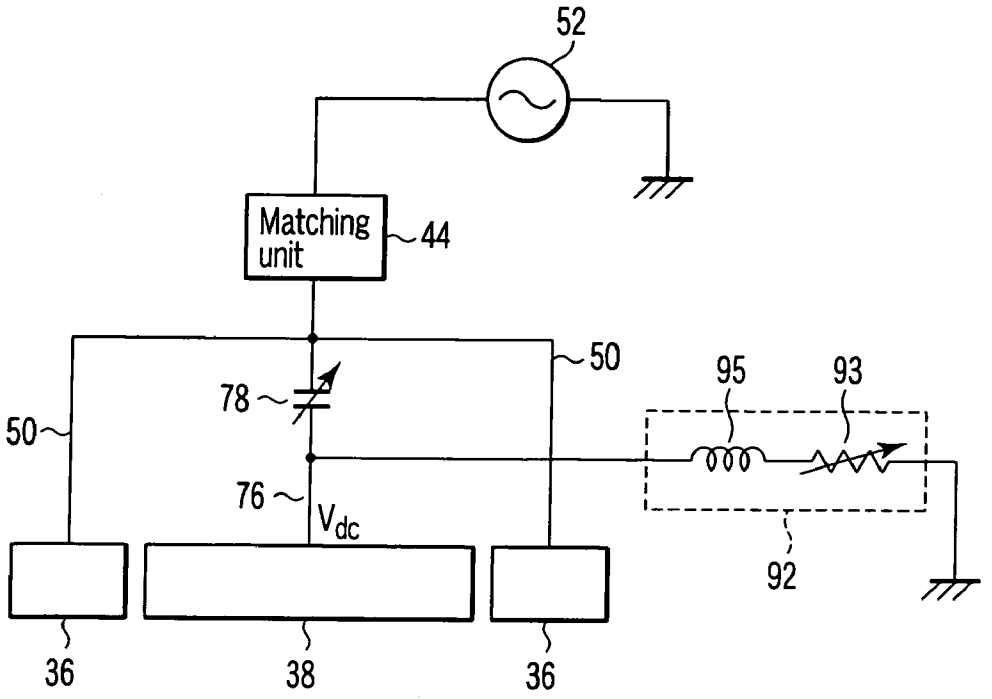

FIG. 15A

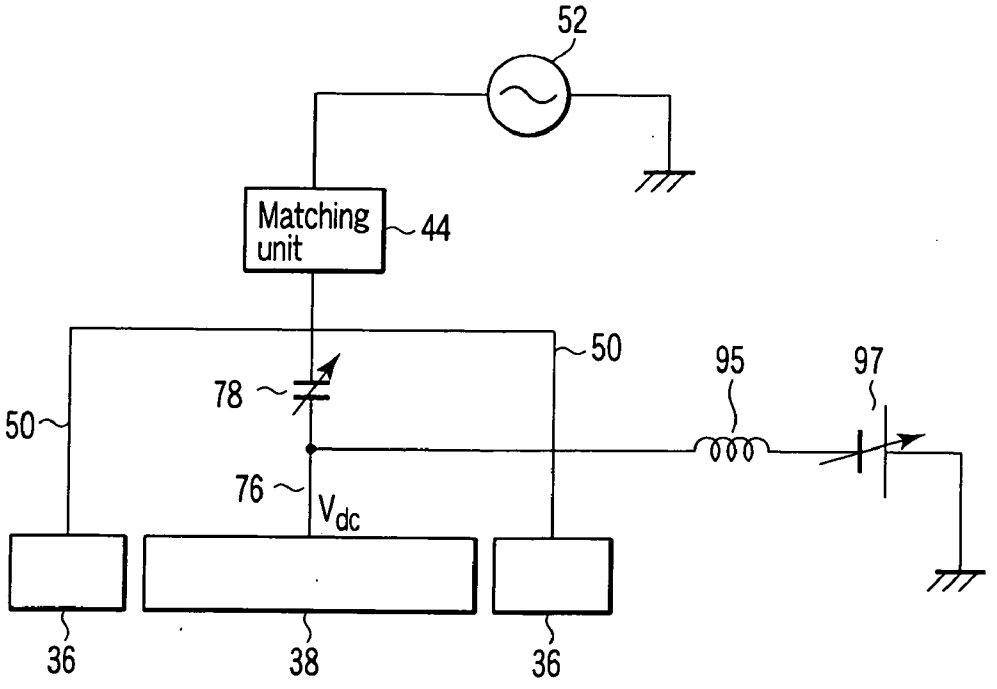

FIG. 15B

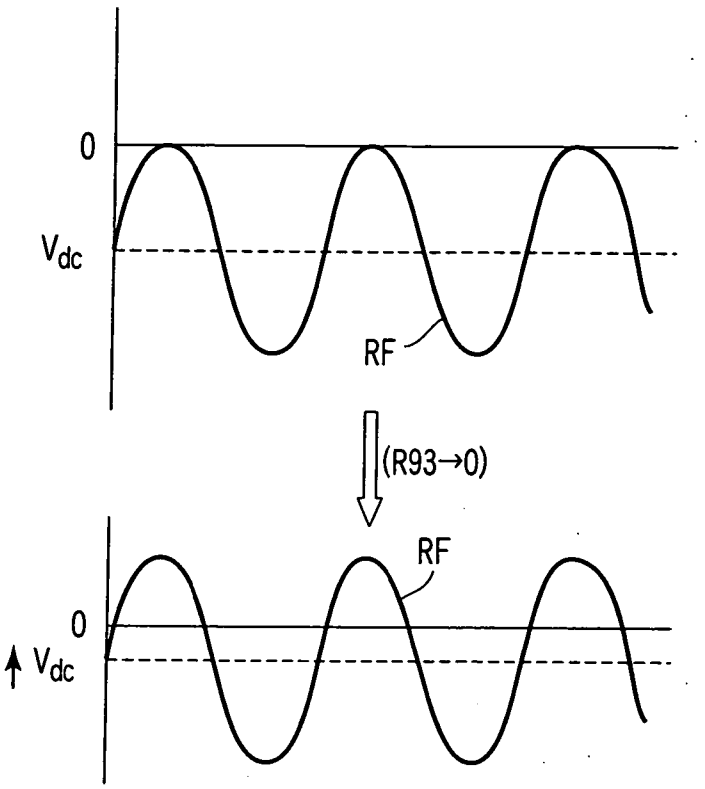
0
V_{dc}
RF
(R93→0)
RF
0
V_{dc}

FIG. 16

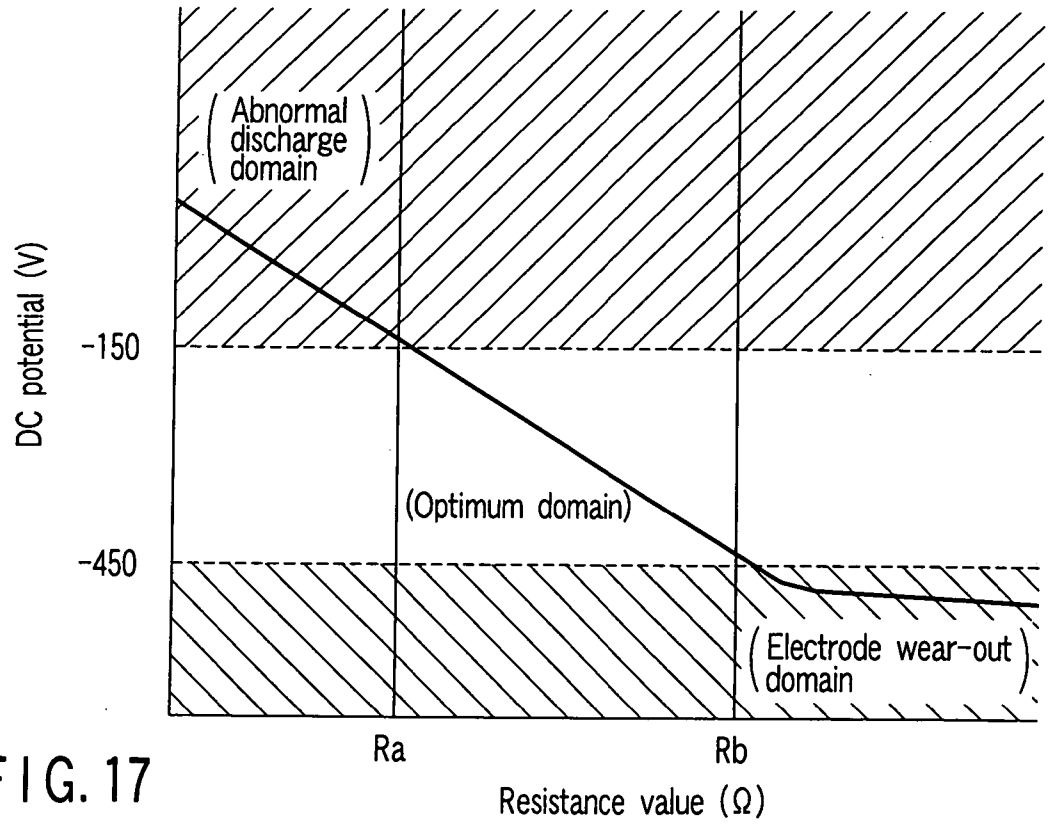
Abnormal discharge domain
DC potential (V)
-150
(Optimum domain)
-450
Electrode wear-out domain
Ra
Rb
Resistance value (Ω)

FIG. 17

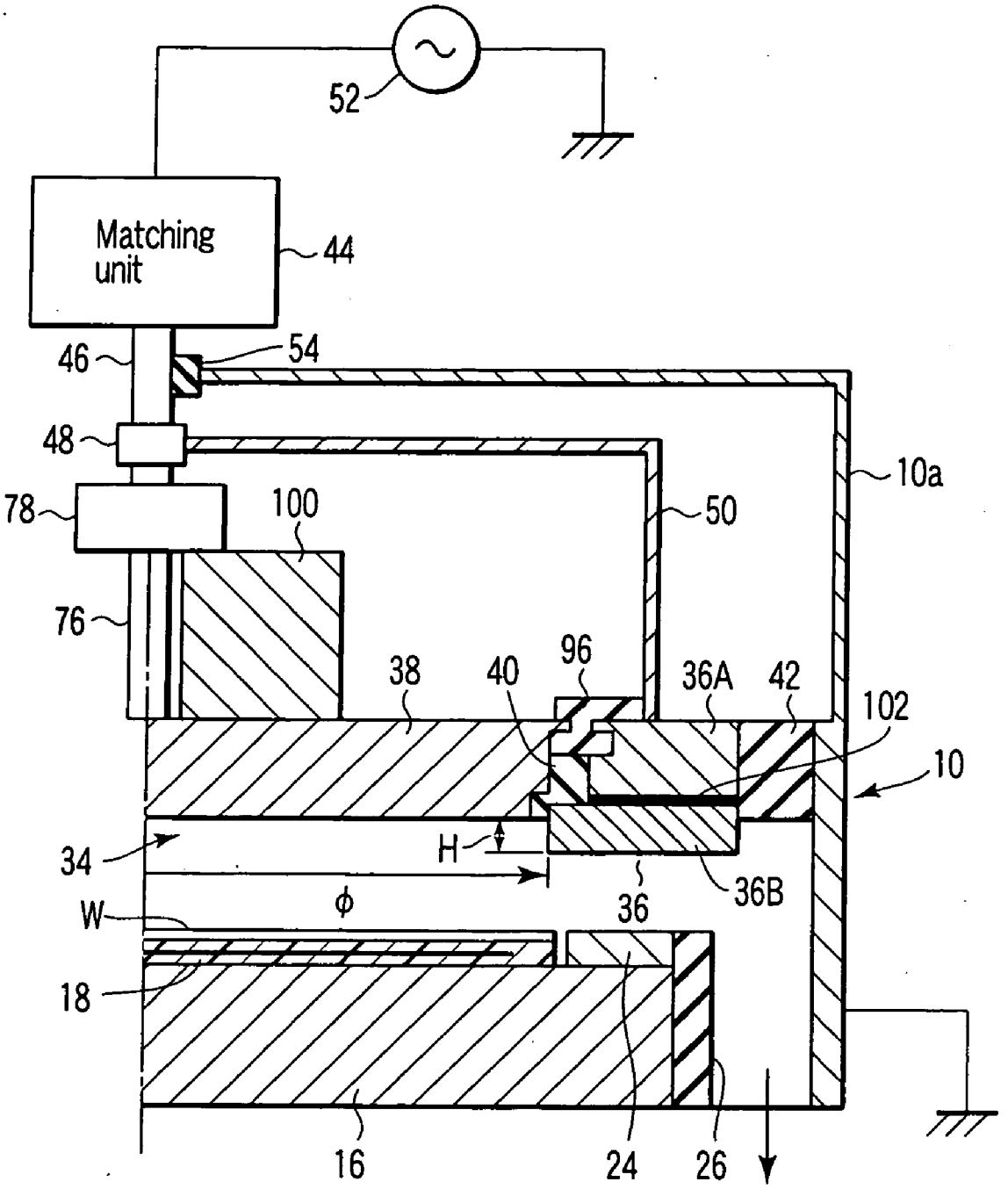
52
Matching unit
44
46
54
48
78
100
50
10a
76
38
40
96
36A
42
102
10
34
H
36B
W
ϕ
36
18
16
24
26

FIG. 18

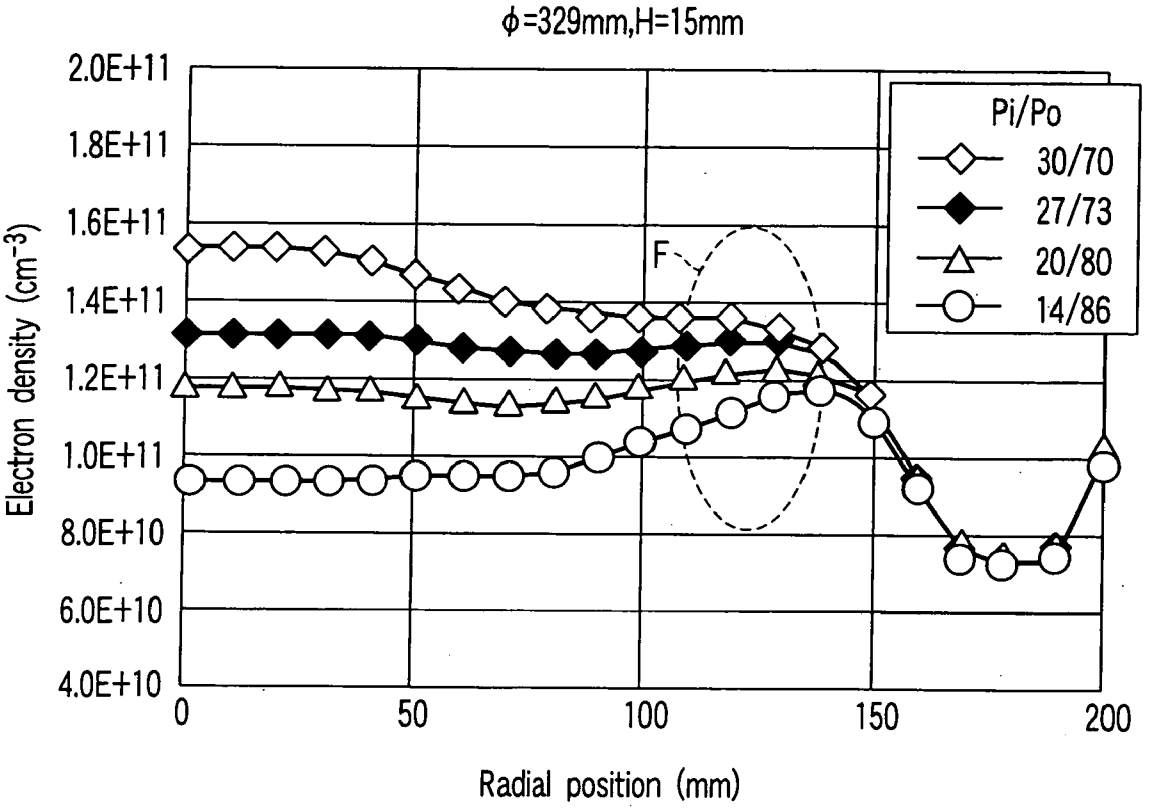
ϕ=329mm,H=15mm
2.0E+11
1.8E+11
1.6E+11
1.4E+11
1.2E+11
1.0E+11
8.0E+10
6.0E+10
4.0E+10
Electron density (cm-3)
0
50
100
150
200
Radial position (mm)
F
Pi/Po
30/70
27/73
20/80
14/86

FIG. 19A

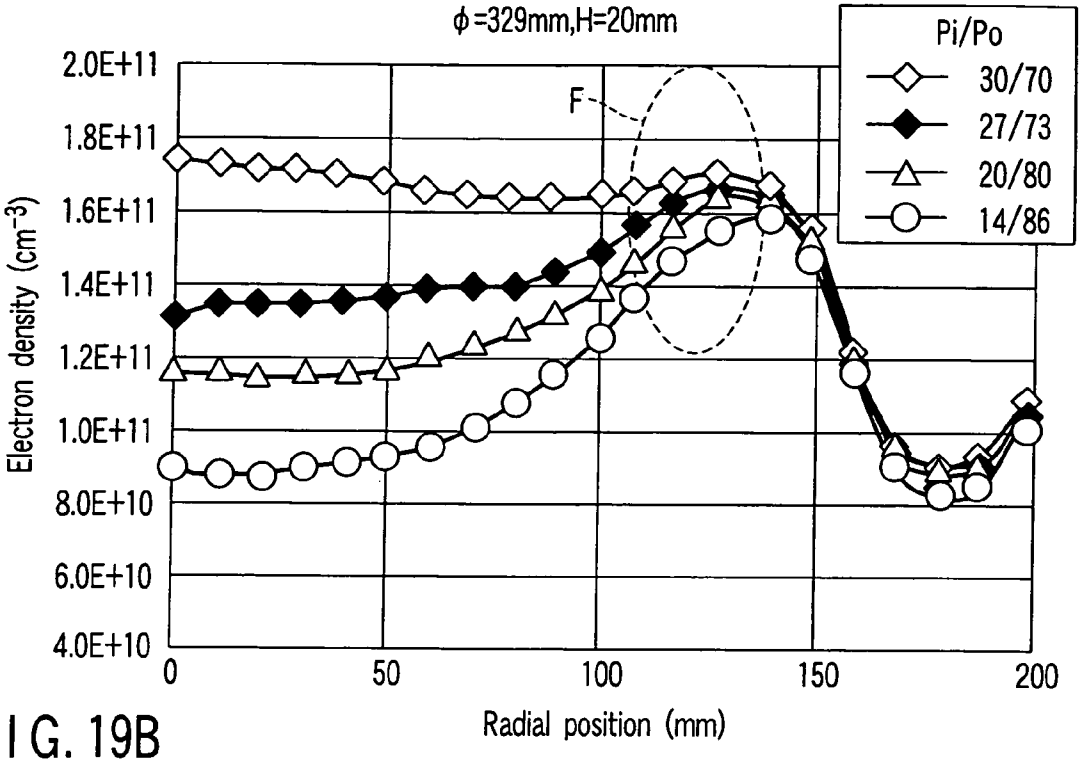

FIG. 19B

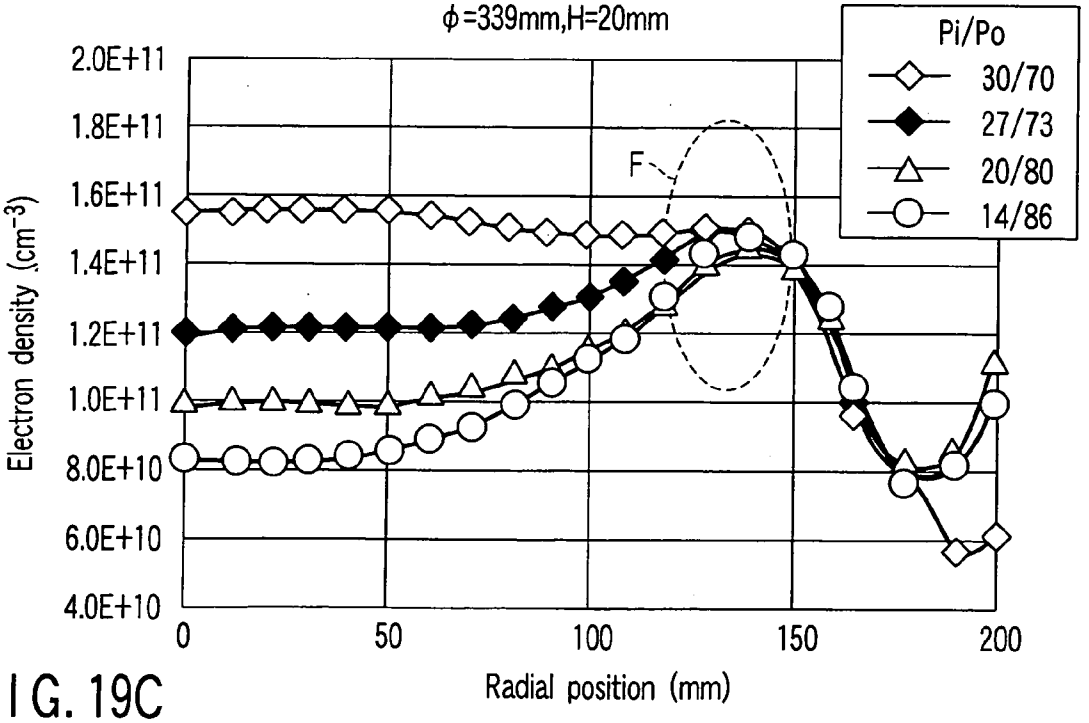

FIG. 19C

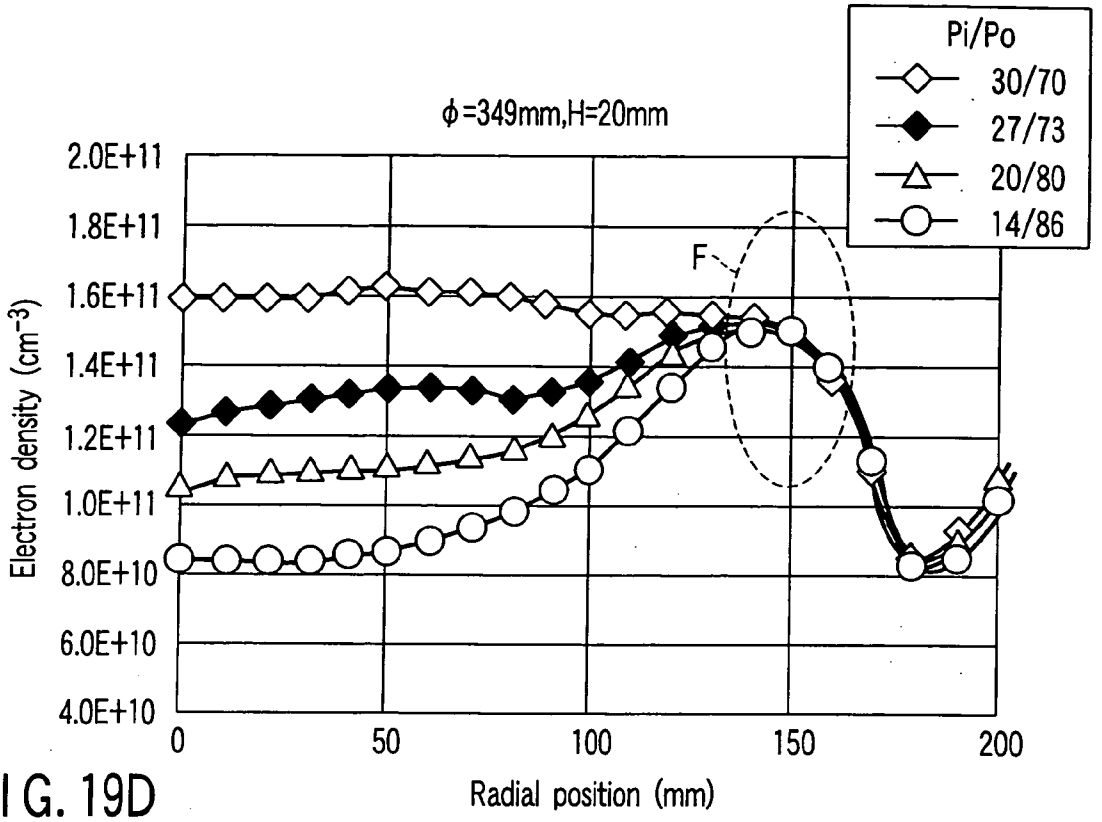

FIG. 19D

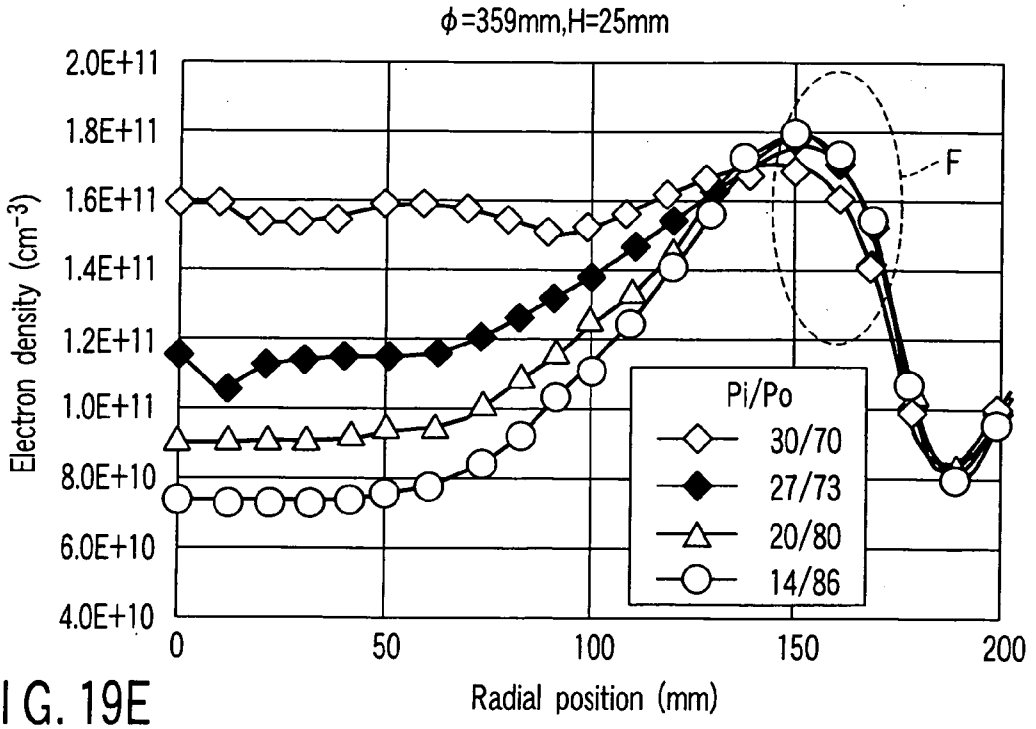

FIG. 19E

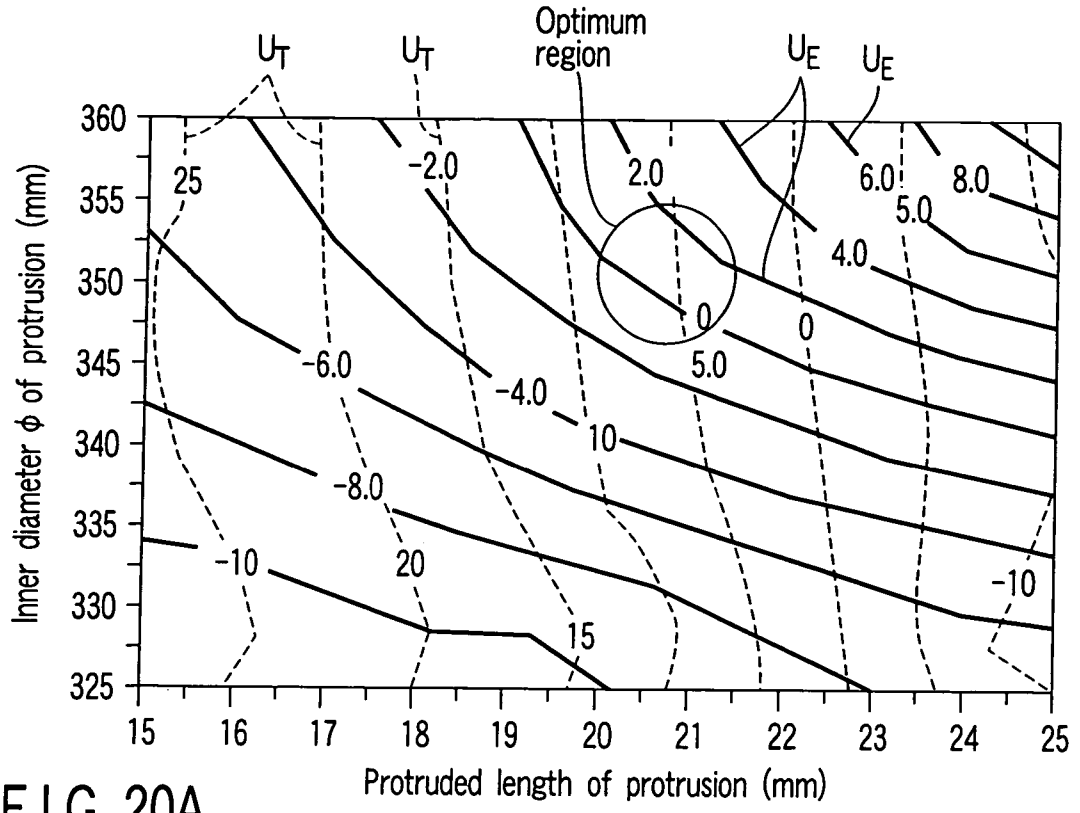

FIG. 20A

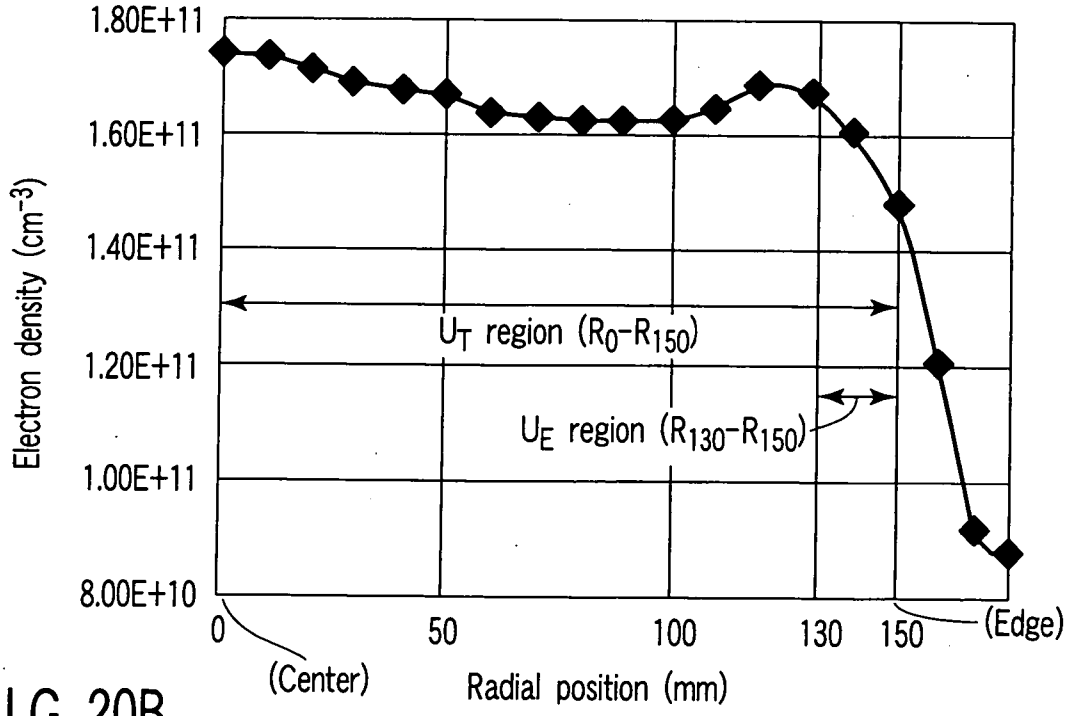

FIG. 20B

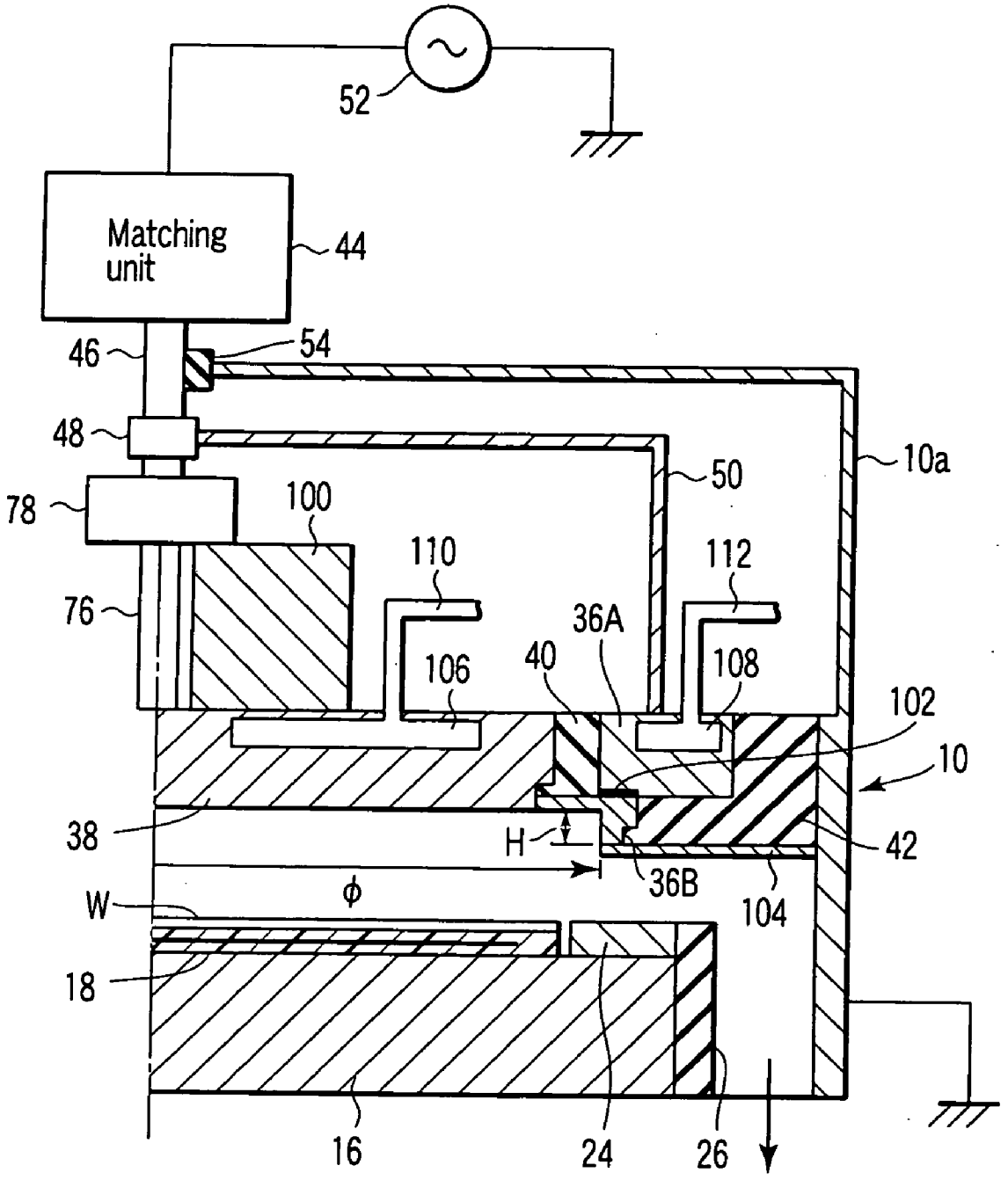
52
Matching unit
44
46
54
48
50
10a
78
100
110
112
76
36A
106
40
108
102
10
38
H
42
36B
W
ϕ
104
18
16
24
26

FIG. 21

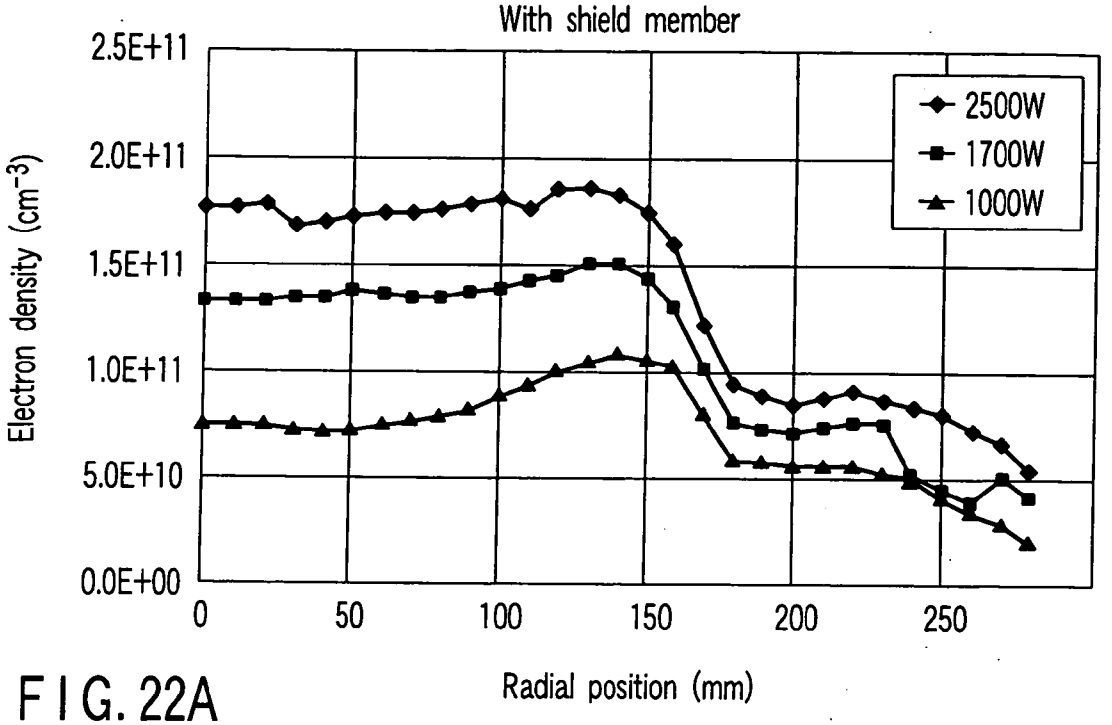

FIG. 22A

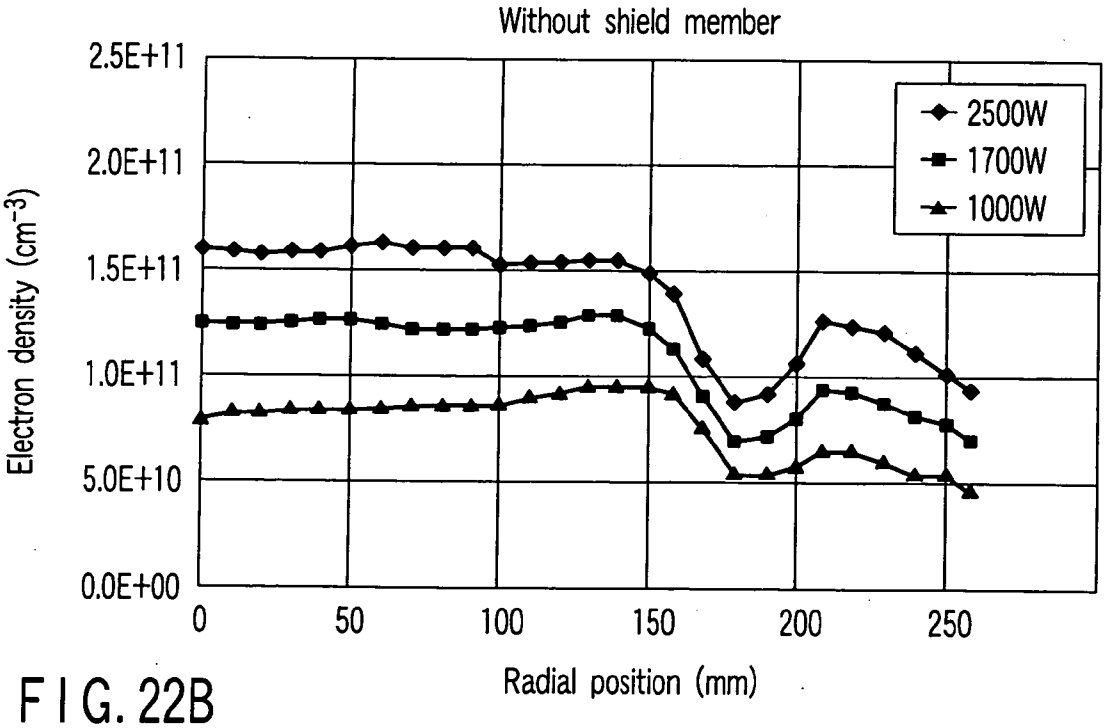

FIG. 22B

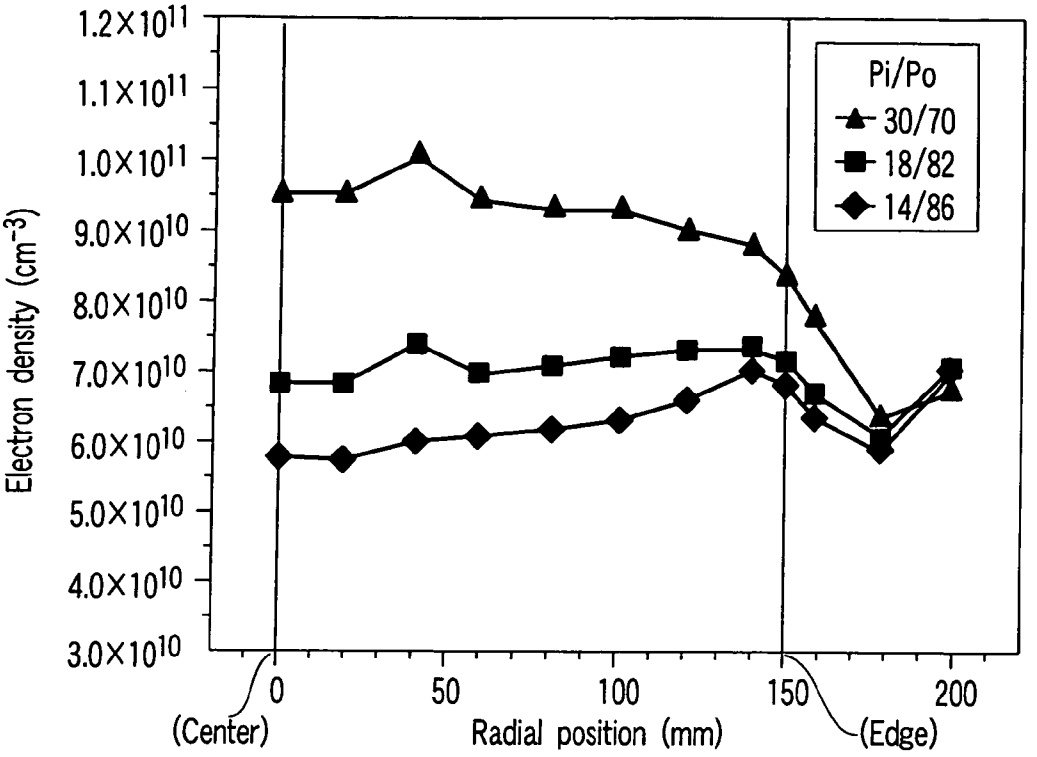
Electron density (cm^{-3})
1.2X10^11
1.1X10^11
1.0X10^11
9.0X10^10
8.0X10^10
7.0X10^10
6.0X10^10
5.0X10^10
4.0X10^10
3.0X10^10
Pi/Po
30/70
18/82
14/86
0
50
100
150
200
(Center)
Radial position (mm)
(Edge)

FIG. 23

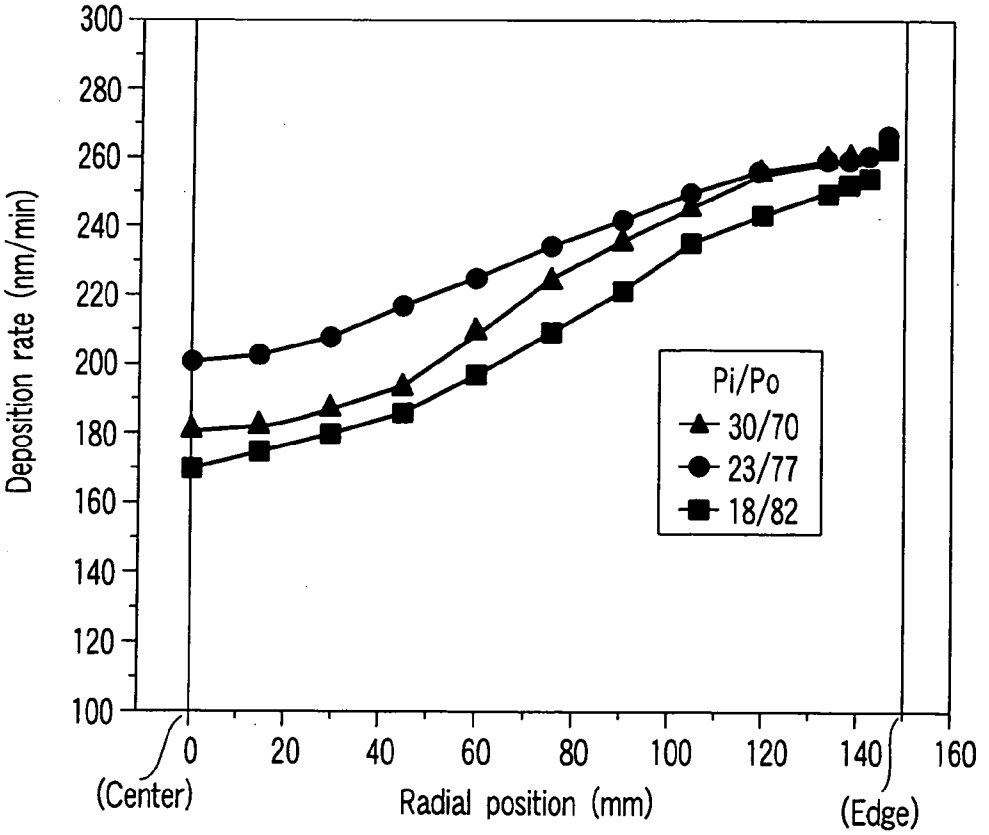
Deposition rate (nm/min)
300
280
260
240
220
200
180
160
140
120
100
Pi/Po
30/70
23/77
18/82
0
20
40
60
80
100
120
140
160
(Center)
Radial position (mm)
(Edge)

FIG. 24

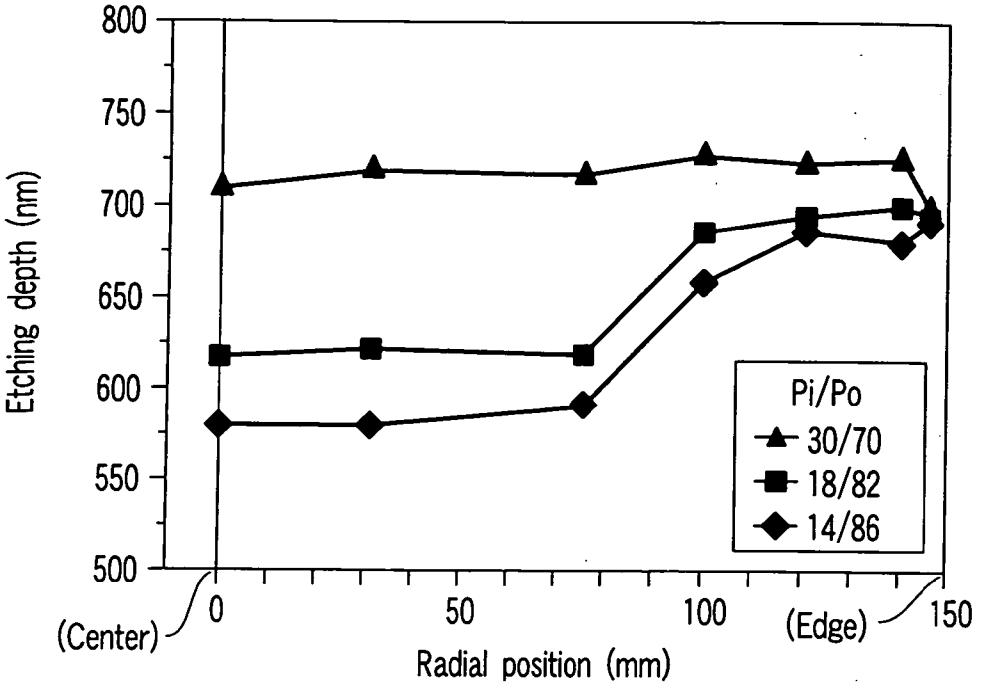
800
750
700
650
600
550
500
Etching depth (nm)
Pi/Po
30/70
18/82
14/86
(Center)
0
50
100
(Edge)
150
Radial position (mm)

FIG. 25

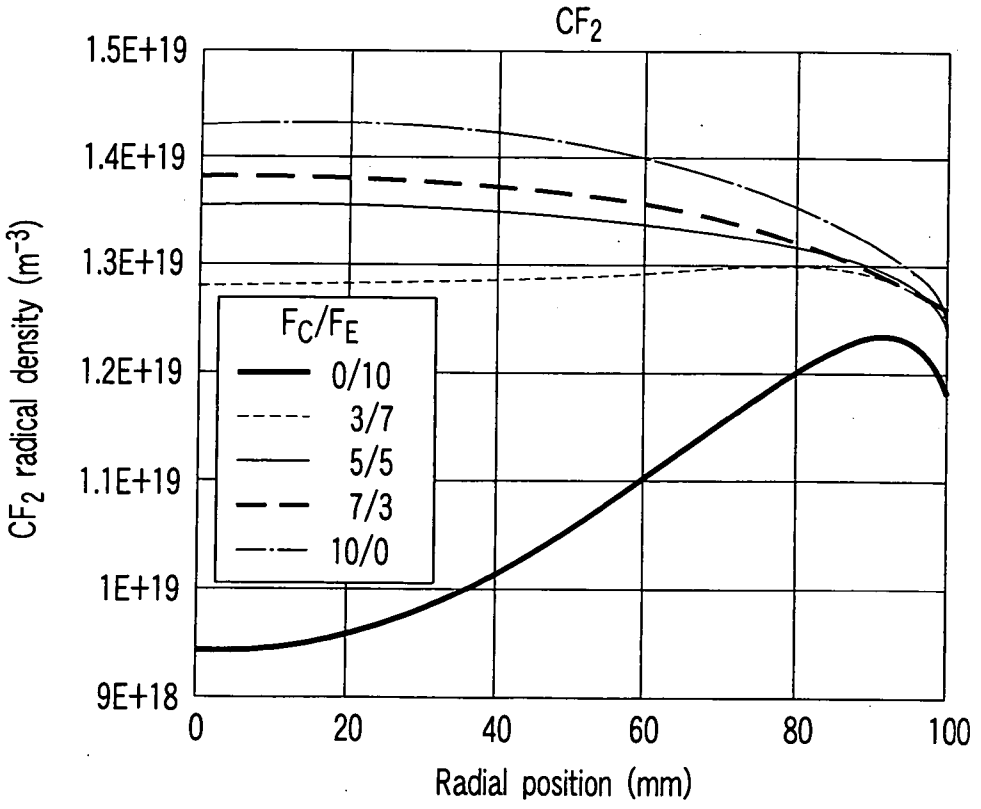
CF_2
1.5E+19
1.4E+19
1.3E+19
1.2E+19
1.1E+19
1E+19
9E+18
CF_2 radical density (m^{-3})
F_C/F_E
0/10
3/7
5/5
7/3
10/0
0
20
40
60
80
100
Radial position (mm)

FIG. 26

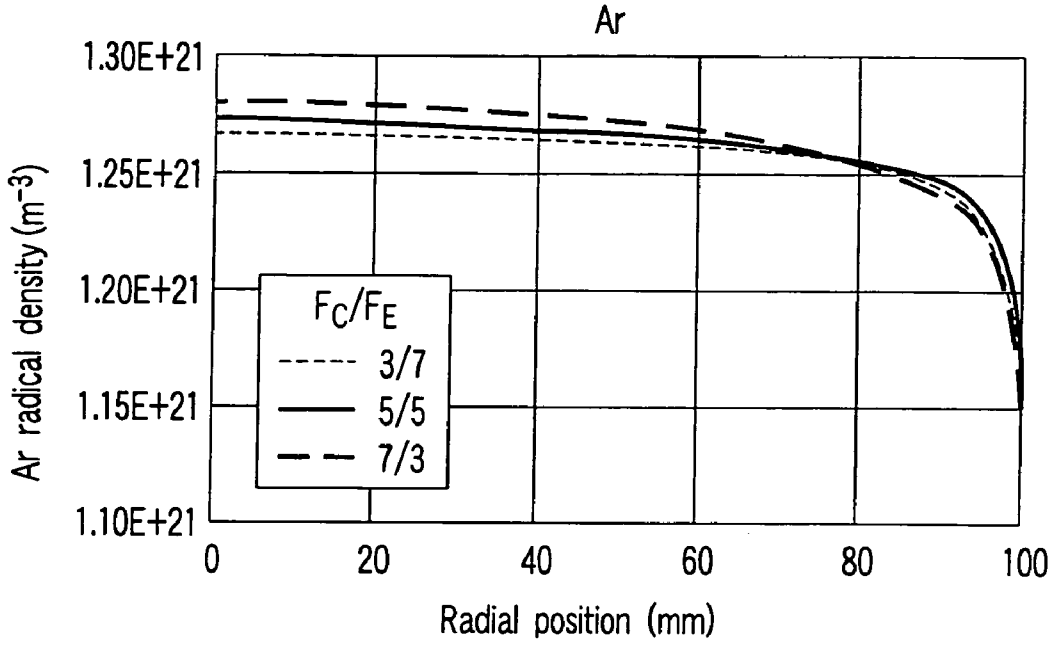
Ar
1.30E+21
1.25E+21
1.20E+21
1.15E+21
1.10E+21
Ar radical density (m^{-3})
F_C/F_E
3/7
5/5
7/3
0
20
40
60
80
100
Radial position (mm)

FIG. 27

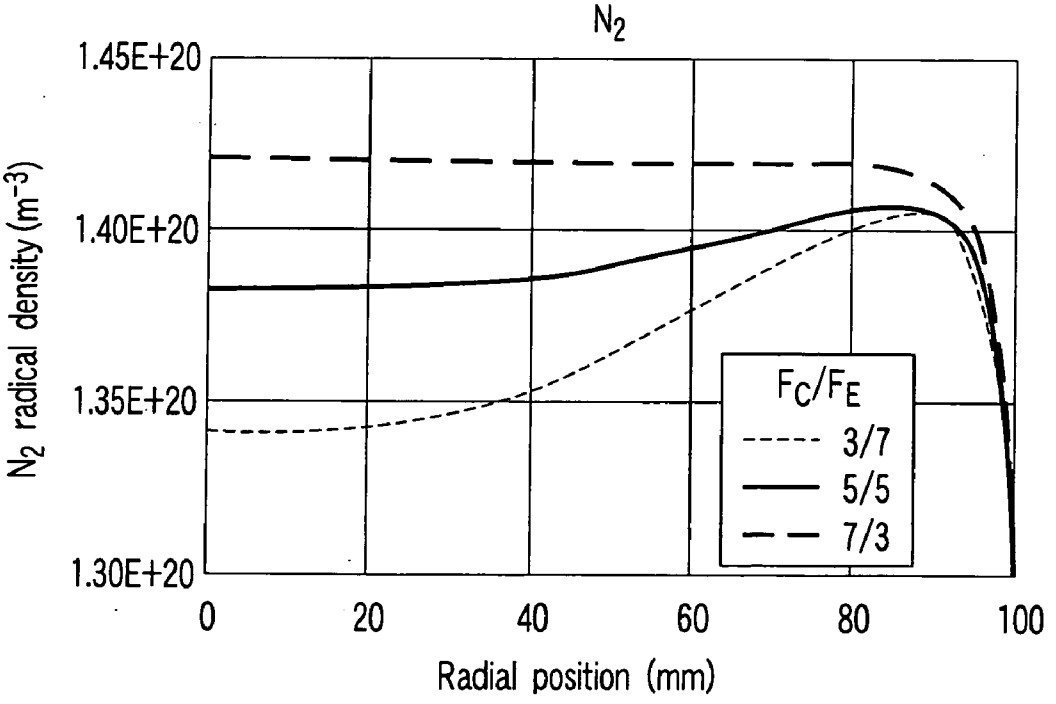
N_2
1.45E+20
1.40E+20
1.35E+20
1.30E+20
N_2 radical density (m^{-3})
F_C/F_E
3/7
5/5
7/3
0
20
40
60
80
100
Radial position (mm)

FIG. 28

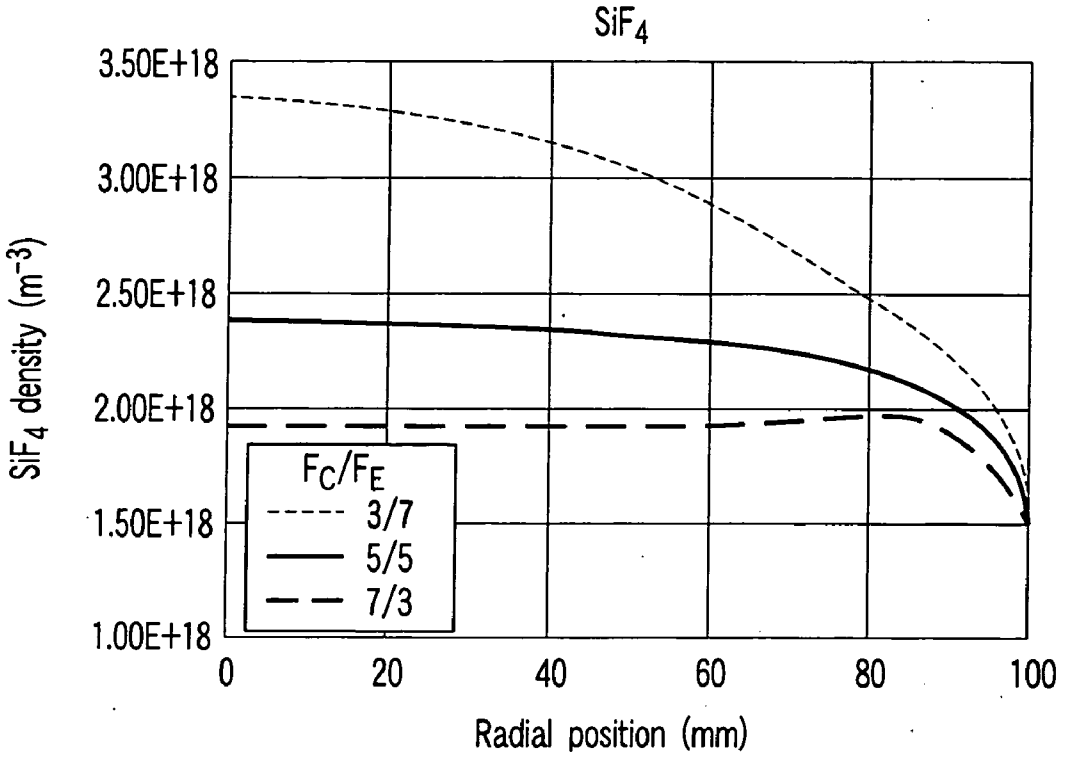
SiF4
3.50E+18
3.00E+18
2.50E+18
2.00E+18
1.50E+18
1.00E+18
SiF4 density (m-3)
FC/FE
3/7
5/5
7/3
0
20
40
60
80
100
Radial position (mm)

FIG. 29

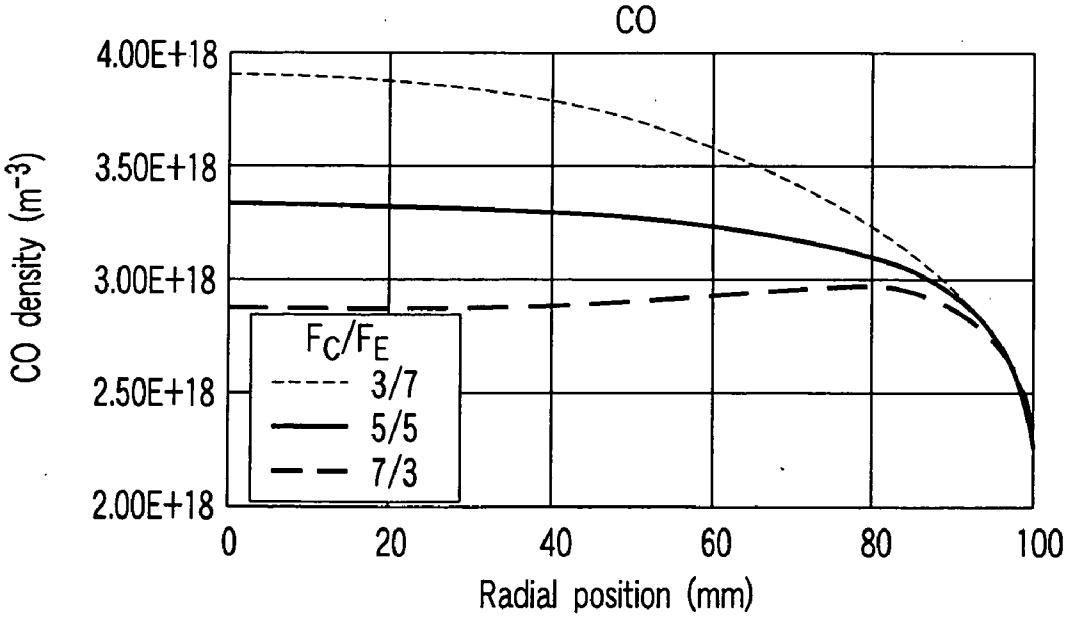
CO
4.00E+18
3.50E+18
3.00E+18
2.50E+18
2.00E+18
CO density (m-3)
FC/FE
3/7
5/5
7/3
0
20
40
60
80
100
Radial position (mm)

FIG. 30

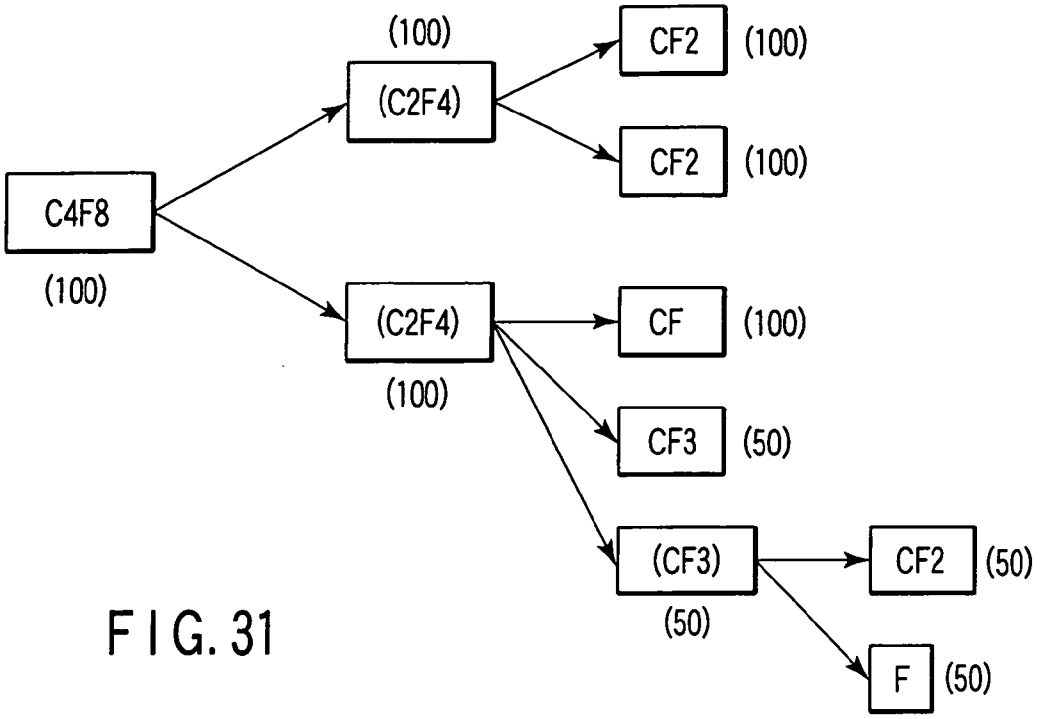

FIG. 31

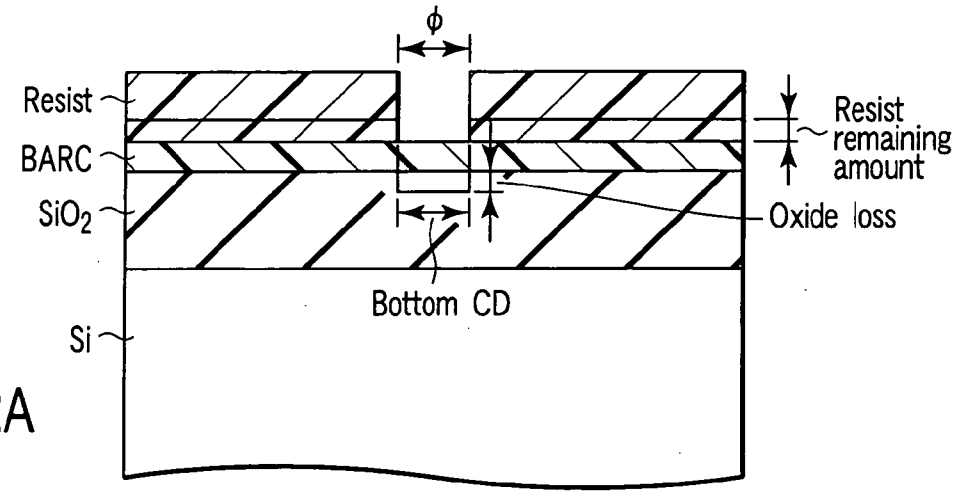

FIG. 32A

F_C/F_E=50/50

FIG. 32B

	Oxide loss (nm)	Bottom CD (nm)	Resist remaining amount (nm)
Center	45.2	127.4	123.3
Edge	39	199	216

F_C/F_E=70/30

	Oxide loss (nm)	Bottom CD (nm)	Resist remaining amount (nm)
Center	39	125.3	216
Edge	39	125.3	216

FIG. 32C

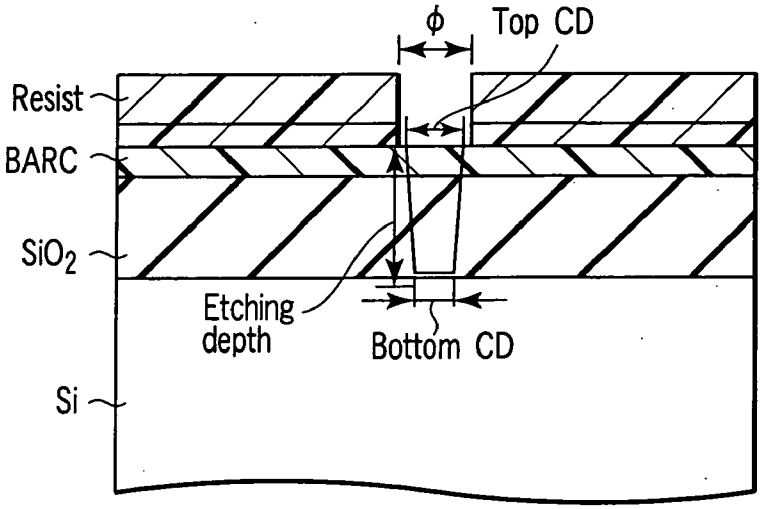

FIG. 33A

F_C/F_E=50/50

	Etching depth (nm)	Top CD (μm)	Bottom CD (μm)	Bottom/ top ratio (%)
Center	861	0.186	0.107	57.5
Edge	762	0.181	0.110	60.8

FIG. 33B

F_C/F_E=10/90

	Etching depth (nm)	Top CD (μm)	Bottom CD (μm)	Bottom/ top ratio (%)
Center	770	0.173	0.130	75.1
Edge	758	0.161	0.122	75.8

FIG. 33C

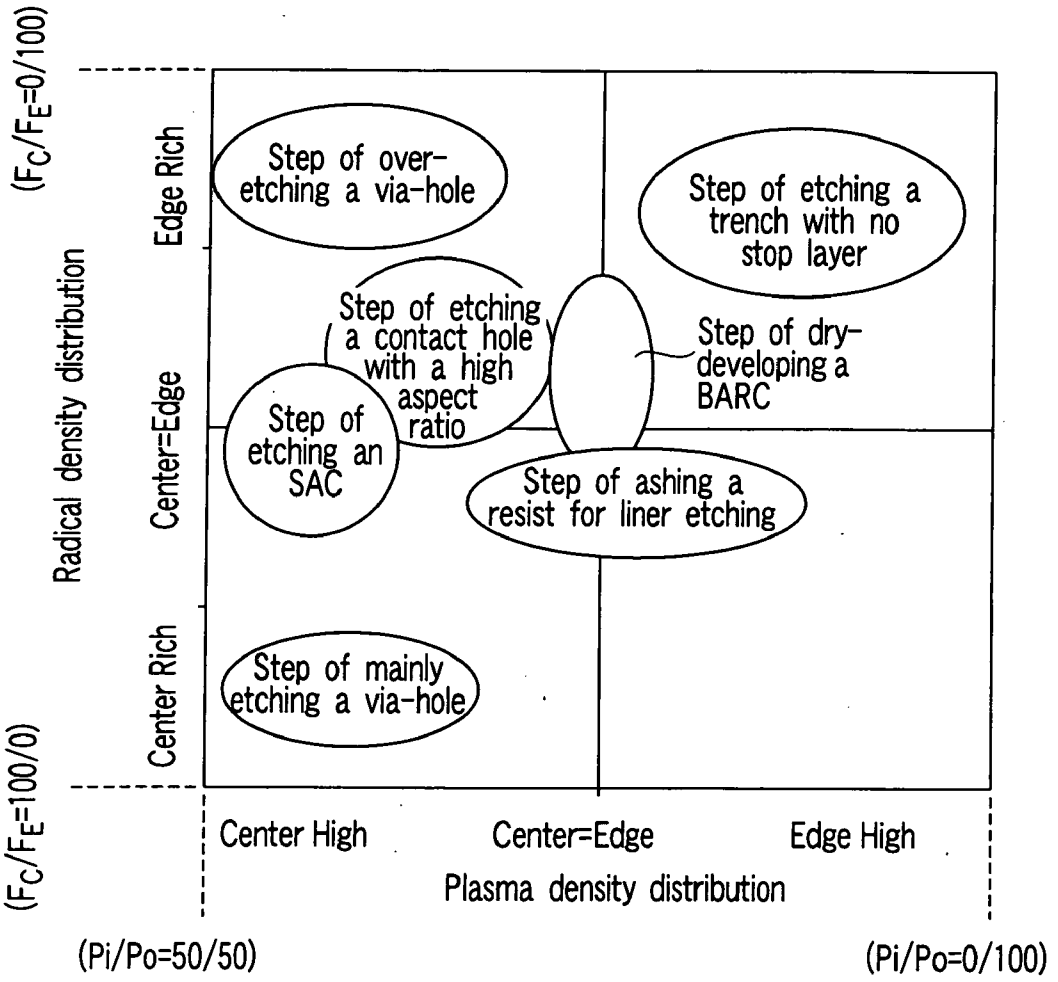

FIG. 34

PLASMA PROCESSING METHOD AND APPARATUS

CROSS REFERENCE TO RELATED APPLICATIONS

[0001] This is a Continuation Application of PCT Application No. PCT/JP03/15029, filed Nov. 25, 2003, which was published under PCT Article 21(2) in Japanese.

[0002] This application is based upon and claims the benefit of priority from prior Japanese Patent Applications No. 2002-341949, filed Nov. 26, 2002; and No. 2003-358432, filed Oct. 17, 2003, the entire contents of both of which are incorporated herein by reference.

BACKGROUND OF THE INVENTION

[0003] 1. Field of the Invention

[0004] The present invention relates to a technique for subjecting a target substrate to a plasma process, and specifically to a plasma processing technique for processing a substrate, using radicals and ions derived from plasma. Particularly, the present invention relates to a plasma processing technique utilized in a semiconductor process for manufacturing semiconductor devices. The term "semiconductor process" used herein includes various kinds of processes which are performed to manufacture a semiconductor device or a structure having wiring layers, electrodes, and the like to be connected to a semiconductor device, on a target substrate, such as a semiconductor wafer or a glass substrate used for an LCD (Liquid Crystal Display) or FPD (Flat Panel Display), by forming semiconductor layers, insulating layers, and conductive layers in predetermined patterns on the target substrate.

[0005] 2. Description of the Related Art

[0006] In manufacturing semiconductor devices and FPDs, plasma is often used for processes, such as etching, deposition, oxidation, and sputtering, so that process gases can react well at a relatively low temperature. Parallel-plate plasma processing apparatuses of the capacitive coupling type are in the mainstream of plasma processing apparatuses of the single substrate type.

[0007] In general, a parallel-plate plasma processing apparatus of the capacitive coupling type includes a process container or reaction chamber configured to reduce the pressure therein, and an upper electrode and a lower electrode disposed therein in parallel with each other. The lower electrode is grounded and configured to support a target substrate (semiconductor wafer, glass substrate, or the like) thereon. The upper electrode and/or lower electrode are supplied with RF voltage through a matching unit. At the same time, a process gas is delivered from a showerhead provided on the upper electrode side. Electrons are accelerated by an electric field formed between the upper electrode and lower electrode and collide with the process gas, thereby ionizing the gas and generating plasma. Neutral radicals and ions derived from the plasma are used to perform a predetermined micro-fabrication on the surface of the substrate. In the process described above, the two electrodes function to form a capacitor.

[0008] The majority of ions in the plasma are positive ions, and the number of positive ions is almost the same as that of electrons. The density of the ions or electrons is far smaller than the density of neutral particles or radicals. In general, plasma etching is arranged to cause radicals and ions to act on the substrate surface at the same time. Radicals perform isotropic etching on the substrate surface by means of chemical reactions. Ions are accelerated by an electric field and vertically incident on the substrate surface, and perform vertical (anisotropic) etching on the substrate surface by means of physical actions.

[0009] Conventional plasma processing apparatuses are arranged to cause radicals and ions generated in plasma to act on the substrate surface with the same density distribution. In other words, where the radical density is higher at the substrate central portion than at the substrate peripheral portion, the ion density (i.e., electron density or plasma density) is also higher at the substrate central portion than at the substrate peripheral portion. Particularly, in parallel-plate plasma processing apparatuses described above, if the frequency of the RF applied to the upper electrode is set higher, when the RF is supplied from an RF power supply through a feed rod to the electrode backside, it is transmitted through the electrode surface by means of the skin effect and is concentrated at the central portion of the electrode bottom surface (plasma contact surface). As a consequence, the electric field intensity at the central portion of the electrode bottom surface becomes higher than the electric field intensity at the peripheral portion, so both the radical density and ion density (electron density) become higher at the electrode central portion than at the electrode peripheral portion. However, if radicals and ions are always limited or restricted to such a relationship that they have the same distribution in acting on the substrate surface, it is difficult to perform a predetermined plasma process on the substrate, and it is particularly difficult to improve the uniformity in process state or process result.

BRIEF SUMMARY OF THE INVENTION

[0010] An object of the present invention is to provide a plasma processing apparatus and method, which can optimize a plasma process in which radicals and ions act on a target substrate at the same time.

[0011] According to a first aspect of the present invention, there is provided a plasma processing method comprising:

[0012] exposing a target substrate to plasma of a predetermined process gas; and

[0013] subjecting the substrate to a predetermined plasma process by the plasma,

[0014] wherein spatial distribution of density of the plasma and spatial distribution of density of radicals in the plasma are controlled independently of each other relative to the substrate to form a predetermined process state over an entire target surface of the substrate.

[0015] According to a second aspect of the present invention, there is provided a plasma processing apparatus arranged to turn a process gas into plasma in a plasma generation space within a process container configured to have a vacuum atmosphere therein, and subject a target substrate placed within the plasma generation space to a predetermined plasma process, the apparatus comprising:

[0016] a plasma density control section configured to control spatial distribution of density of the plasma relative to the substrate; and

[0017] a radical density control section configured to control spatial distribution of density of radicals in the plasma relative to the substrate independently of the plasma density spatial distribution.

[0018] According to the first and second aspects, the spatial distribution of plasma density (i.e., electron density or ion density) and the spatial distribution of radical density are controlled independently of each other relative to the target substrate to optimize the balance or synergy between radical base etching and ion base etching.

[0019] In order to achieve this, the facing portion opposite the target substrate may comprise first and second RF discharge regions configured to control the plasma density spatial distribution, and first and second process gas delivery regions configured to control the radical density spatial distribution, in layouts independently of each other. In this case, by adjusting the balance (ratio) of the RF electric field intensity or input power between the first and second RF discharge regions, the spatial distribution of plasma density (ion density) can be controlled. Further, by adjusting the balance (ratio) of the gas flow rate between the first and second process gas delivery regions, the spatial distribution of radical density can be controlled. If the first and second RF discharge regions respectively agree with or correspond to the first and second process gas delivery regions, change in the input power ratio affects the spatial distribution of radical density, while change in the gas flow-rate ratio affects the spatial distribution of plasma density (ion density). By contrast, where the division layout of the RF discharge regions and the division layout of the process gas delivery regions are independent of each other, such an interlinking relationship is cut off, so that the plasma density distribution and radical density distribution can be controlled independently of each other.

[0020] In one design according to this independent type layout, the facing portion may be divided into two regions as the first and second RF discharge regions on a peripheral side and a central side, respectively, in a radial direction relative to a center through which a vertical line extending from a center of the target substrate passes. Further, the second RF discharge region on the facing portion may be divided into two regions as the first and second process gas delivery regions on a peripheral side and a central side, respectively, in the radial direction. More preferably, the first RF discharge region is disposed radially outside the outer peripheral edge of the target substrate.

[0021] With this layout, the control over the plasma density spatial distribution performed by adjusting the ratio of electric field intensity or input power between the first and second RF discharge regions does not have a substantial influence on the control over the radical density spatial distribution performed by adjusting the ratio of process gas flow rate between the first and second process gas delivery regions. Specifically, the process gas delivered from the first and second process gas delivery regions is dissociated within an area corresponding to the second RF discharge region. Thus, where the balance of electric field intensity or input power between the first and second RF discharge regions is changed, the balance of radical generation amount or density between the first and second process gas delivery regions is not substantially affected. As a consequence, the plasma density spatial distribution and radical density spatial distribution can be controlled independently of each other.

[0022] In one design, an RF output from a single RF power supply may be divided at a predetermined ratio, and thereby discharged from the first RF discharge region and the second RF discharge region. Further, a process gas supplied from a single process gas supply source may be divided at a predetermined ratio, and thereby delivered from the first process gas delivery region and the second process gas delivery region. In this case, the process gas may be delivered from the first and second process gas delivery regions at substantially deferent flow rates per unit area. Where the process gas is a mixture gas of a plurality of gases, the plurality of gases may be delivered from the first process gas delivery region at a first gas mixture ratio, and the plurality of gases may be delivered from the second process gas delivery region at a second gas mixture ratio different from the first gas mixture ratio.

[0023] In one design, processing rates at respective positions on the target surface of the target substrate may be mainly controlled in accordance with the plasma density spatial distribution. Further, one or both of processing selectivity and processing shapes at respective positions on the target surface of the target substrate may be mainly controlled in accordance with the radical density spatial distribution.

[0024] In the plasma processing apparatus according to the second aspect, the plasma density control section may comprise an RF distributor configured to divide and transmit an RF with a constant frequency, output from an RF power supply, at a predetermined ratio to the first and second RF discharge regions. The radical density control section may comprise a process gas distributor configured to divide and supply the process gas, output from a process gas supply source, at a predetermined ratio to the first and second process gas delivery regions. In this case, the RF distributor preferably includes an impedance control section configured to variably control one or both of an impedance of a first feed circuit from the RF power supply to the first RF discharge region, and an impedance of a second feed circuit from the RF power supply to the second RF discharge region. The first and second RF discharge regions may respectively comprise first and second electrodes electrically insulated from each other. The first and second process gas delivery regions preferably include a number of process gas delivery holes formed on the second electrode.

[0025] According to the first and second aspects, it is possible to optimize a plasma process arranged to cause radicals and ions to act on a target substrate at the same time.

[0026] Additional objects and advantages of the invention will be set forth in the description which follows, and in part will be obvious from the description, or may be learned by practice of the invention. The objects and advantages of the invention may be realized and obtained by means of the instrumentalities and combinations particularly pointed out hereinafter.

BRIEF DESCRIPTION OF THE SEVERAL VIEWS OF THE DRAWING

[0027] The accompanying drawings, which are incorporated in and constitute a part of the specification, illustrate embodiments of the invention, and together with the general description given above and the detailed description of the embodiments given below, serve to explain the principles of the invention.

[0028] **FIG. 1** is a sectional side view showing a plasma etching apparatus according to a first embodiment of the present invention;

[0029] **FIG. 2** is an enlarged partial side view showing a main part of the plasma etching apparatus shown in **FIG. 1**;

[0030] **FIG. 3** is a circuit diagram showing an equivalent circuit of a main part of plasma generating means according to the first embodiment;

[0031] **FIG. 4** is a graph showing distribution characteristics of electric field intensity (relative value), obtained by a function of adjusting the balance of electric field intensity according to the first embodiment;

[0032] **FIG. 5** is a graph showing ratio characteristics of electric field intensity, obtained by a function of adjusting the balance of electric field intensity according to the first embodiment;

[0033] **FIGS. 6A and 6B** are graphs showing spatial distribution characteristics of electron density according to the first embodiment;

[0034] **FIGS. 7A and 7B** are graphs showing spatial distribution characteristics of etching rate according to the first embodiment;

[0035] **FIG. 8** is a sectional side view showing a plasma etching apparatus according to a second embodiment of the present invention;

[0036] **FIGS. 9A and 9B** are graphs showing spatial distribution characteristics of etching rate according to the second embodiment;

[0037] **FIGS. 10A and 10B** are graphs showing spatial distribution characteristics of etching rate according to the second embodiment;

[0038] **FIG. 11** is a graph showing characteristics of variable capacitance vs. inner input power according to the second embodiment;

[0039] **FIG. 12** is a circuit diagram showing an equivalent circuit of a plasma generation RF feed circuit according to the second embodiment;

[0040] **FIG. 13** is a view showing an effect of a conductive member disposed around an upper feed rod according to the second embodiment;

[0041] **FIG. 14** is a graph showing characteristics of variable capacitance vs. bottom self-bias voltage according to the second embodiment;

[0042] **FIGS. 15A and 15B** are circuit diagrams each showing the circuit structure of a low-pass filter according to the second embodiment;

[0043] **FIG. 16** is a diagram showing an effect of resistance provided in a low-pass filter according to the second embodiment;

[0044] **FIG. 17** is a graph showing the optimum range of resistance provided in a low-pass filter according to the second embodiment;

[0045] **FIG. 18** is a sectional side view showing a main part of the plasma etching apparatus according to the second embodiment;

[0046] **FIGS. 19A** to **19E** are graphs showing spatial distribution characteristics of electron density, using as parameters the inner diameter and protruded length of an upper electrode protrusion according to the second embodiment;

[0047] **FIGS. 20A and 20B** are graphs showing characteristic lines of electron density uniformity, using as two-dimensional parameters the inner diameter and protruded length of an upper electrode protrusion according to the second embodiment;

[0048] **FIG. 21** is a sectional side view showing a plasma etching apparatus according to a third embodiment of the present invention;

[0049] **FIGS. 22A and 22B** are graphs showing spatial distribution characteristics of electron density to demonstrate an effect of a shield member according to the third embodiment;

[0050] **FIG. 23** is a graph showing spatial distribution characteristics of electron density, using inner/outer input power ratio as a parameter, according to a fourth embodiment of the present invention;

[0051] **FIG. 24** is a graph showing spatial distribution characteristics of polymer film deposition rate, using inner/outer input power ratio as a parameter, according to the fourth embodiment;

[0052] **FIG. 25** is a graph showing spatial distribution characteristics of etching depth, using inner/outer input power ratio as a parameter, according to the fourth embodiment;

[0053] **FIG. 26** is a graph showing spatial distribution characteristics of CF_2 radical density, using center/periphery gas flow-rate ratio as a parameter, according to a fifth embodiment of the present invention;

[0054] **FIG. 27** is a graph showing spatial distribution characteristics of Ar radical density, using center/periphery gas flow-rate ratio as a parameter, according to the fifth embodiment;

[0055] **FIG. 28** is a graph showing spatial distribution characteristics of N_2 radical density, using center/periphery gas flow-rate ratio as a parameter, according to the fifth embodiment;

[0056] **FIG. 29** is a graph showing spatial distribution characteristics of SiF_4 reaction products, using center/periphery gas flow-rate ratio as a parameter, according to the fifth embodiment;

[0057] **FIG. 30** is a graph showing spatial distribution characteristics of CO reaction products, using center/periphery gas flow-rate ratio as a parameter, according to the fifth embodiment;

[0058] **FIG. 31** is a diagram showing a mechanism of radical generation (dissociation) obtained by a simulation according to the fifth embodiment;

[0059] **FIGS. 32A** to **32C** are views showing an examination model for BARC etching and sets of measurement data according to a sixth embodiment of the present invention;

[0060] **FIGS. 33A** to **33**C are views showing an examination model for SiO_2 etching and sets of measurement data according to a seventh embodiment of the present invention; and

[0061] **FIG. 34** is a diagram showing an application example of independent control over two systems for plasma density distribution and radical density distribution.

DETAILED DESCRIPTION OF THE INVENTION

[0062] Embodiments of the present invention will be described hereinafter with reference to the accompanying drawings. In the following description, the constituent elements having substantially the same function and arrangement are denoted by the same reference numerals, and a repetitive description will be made only when necessary.

First Embodiment

[0063] **FIG. 1** is a sectional side view showing a plasma etching apparatus according to a first embodiment of the present invention. This plasma etching apparatus is structured as a parallel-plate plasma etching apparatus of the capacitive coupling type. The apparatus includes a cylindrical chamber (process container) **10**, which is made of, e.g., aluminum with an alumite-processed (anodized) surface. The chamber **10** is protectively grounded.

[0064] A columnar susceptor pedestal **14** is disposed on the bottom of the chamber **10** through an insulating plate **12** made of, e.g., a ceramic. A susceptor **16** made of, e.g., aluminum is disposed on the susceptor pedestal **14**. The susceptor **16** is used as a lower electrode, on which a target substrate, such as a semiconductor wafer W, is placed.

[0065] The susceptor **16** is provided with an electrostatic chuck **18** on the top, for holding the semiconductor wafer W by an electrostatic attraction force. The electrostatic chuck **18** comprises an electrode **20** made of a conductive film, and a pair of insulating layers or insulating sheets sandwiching the electrode **20**. The electrode **20** is electrically connected to a direct-current (DC) power supply **22**. With a DC voltage applied from the DC power supply **22**, the semiconductor wafer W is attracted and held on the electrostatic chuck **18** by the Coulomb force. A focus ring made of, e.g., silicon is disposed on the top of the susceptor **16** to surround the electrostatic chuck **18** to improve etching uniformity. A cylindrical inner wall member **26** made of, e.g., quartz is attached to the side of the susceptor **16** and susceptor pedestal **14**.

[0066] The susceptor pedestal **14** is provided with a cooling medium space **28** formed therein and annularly extending therethrough. A cooling medium set at a predetermined temperature, such as cooling water, is circulated within the cooling medium space **28** from a chiller unit (not shown) through lines **30***a* and **30***b*. The temperature of the cooling medium is set to control the process temperature of the semiconductor wafer W placed on the susceptor **16**. Further, a heat transmission gas, such as He gas, is supplied from a heat transmission gas supply unit (not shown), through a gas supply line **32**, into the interstice between the top surface of the electrostatic chuck **18** and the bottom surface of the semiconductor wafer W.

[0067] An upper electrode **34** is disposed above the susceptor **16** in parallel with the susceptor. The space between the electrodes **16** and **34** is used as a plasma generation space. The upper electrode **34** defines a surface facing the semiconductor wafer W placed on the susceptor (lower electrode) **16**, and thus this facing surface is in contact with plasma generation space. The upper electrode **34** comprises an outer upper electrode **36** and an inner upper electrode **38**. The outer upper electrode **36** has a ring shape or doughnut shape and is disposed to face the susceptor **16** at a predetermined distance. The inner upper electrode **38** has a circular plate shape and is disposed radially inside the outer upper electrode **36** while being insulated therefrom. In terms of plasma generation, the outer upper electrode **36** mainly works for it, and the inner upper electrode **38** assists it.

[0068] **FIG. 2** is an enlarged partial side view showing a main part of the plasma etching apparatus shown in **FIG. 1**. As shown in **FIG. 2**, the outer upper electrode **36** is separated from the inner upper electrode **38** by an annular gap (slit) of, e.g., 0.25 to 2.0 mm, in which a dielectric body **40** made of, e.g., quartz is disposed. A ceramic body may be disposed in this gap. The two electrodes **36** and **38** with the dielectric body **40** sandwiched therebetween form a capacitor. The capacitance C_{40} of this capacitor is set or adjusted to be a predetermined value, on the basis of the size of the gap and the dielectric constant of the dielectric body **40**. An insulating shield member **42** made of, e.g., alumina (Al_2O_3) and having a ring shape is airtightly interposed between the outer upper electrode **36** and the sidewall of the chamber **10**.

[0069] The outer upper electrode **36** is preferably made of a conductor or semiconductor, such as silicon, having a low resistivity to generate a small Joule heat. The outer upper electrode **36** is electrically connected to a first RF power supply **52** through a matching unit **44**, an upper feed rod **46**, a connector **48**, and a feed cylinder **50**. The first RF power supply **52** outputs an RF voltage with a frequency of 13.5 MHz or more, such as 60 MHz. The matching unit **44** is arranged to match the load impedance with the internal (or output) impedance of the RF power supply **52**. When plasma is generated within the chamber **10**, the matching unit **44** performs control for the load impedance and the output impedance of the RF power supply **52** to apparently agree with each other. The output terminal of the matching unit **44** is connected to the top of the upper feed rod **46**.

[0070] The feed cylinder **50** has a cylindrical or conical shape, or a shape close to it, and formed of a conductive plate, such as an aluminum plate or copper plate. The bottom end of the feed cylinder **50** is connected to the outer upper electrode **36** continuously in an annular direction. The top of the feed cylinder **50** is electrically connected to the bottom of the upper feed rod **46** through the connector **48**. Outside the feed cylinder **50**, the sidewall of the chamber **10** extends upward above the height level of the upper electrode **34** and forms a cylindrical grounded conductive body **10***a*. The top of the cylindrical grounded conductive body **10***a* is electrically insulated from the upper feed rod **46** by a tube-like insulating member **54**. According to this design, the load circuit extending from the connector **48** comprises a coaxial path formed of the feed cylinder **50** and outer upper electrode **36** and the cylindrical grounded conductive body **10***a*, wherein the former members (**36** and **50**) function as a waveguide.

[0071] Returning to **FIG. 1**, the inner upper electrode **38** includes an electrode plate **56** having a number of gas

through-holes **56***a*, and an electrode support **58** detachably supports the electrode plate **56**. The electrode plate **56** is made of a semiconductor material, such as Si or SiC, while the electrode support **58** is made of a conductor material, such as aluminum with an alumite-processed surface. The electrode support **58** has two gas supply cells, i.e., a central gas supply cell **62** and a peripheral gas supply cell **64**, formed therein and separated by an annular partition member **60**, such as an O-ring. The central gas supply cell **62** is connected to some part of a number of gas delivery holes **56***a* formed at the bottom surface, so as to constitute a central showerhead. The peripheral gas supply cell **64** is connected to other part of a number of gas delivery holes **56***a* formed at the bottom surface, so as to constitute a peripheral showerhead.

[**0072**] The gas supply cells **62** and **64** are supplied with a process gas from a common process gas supply source **66** at a predetermined flow-rate ratio. More specifically, a gas supply line **68** is extended from the process gas supply source **66** and divided into two lines **68***a* and **68***b* connected to the gas supply cells **62** and **64**. The branch lines **68***a* and **68***b* are provided with flow control valves **70***a* and **70***b* disposed thereon, respectively. The conductance values of the flow passages from the process gas supply source **66** to the gas supply cells **62** and **64** are equal to each other. Accordingly, the flow-rate ratio of the process gas supplied into the two gas supply cells **62** and **64** is arbitrarily adjusted by adjusting the flow control valves **70***a* and **70***b*. The gas supply line **68** is provided with a mass-flow controller (MFC) **72** and a switching valve **74** disposed thereon.

[**0073**] The flow-rate ratio of the process gas supplied into the central gas supply cell **62** and peripheral gas supply cell **64** is thus adjusted. As a consequence, the ratio (FC/FE) between the gas flow rate FC from the central showerhead and the gas flow rate FE from the peripheral showerhead is arbitrarily adjusted. As described above, the central showerhead is defined by gas through-holes **56***a* at the electrode central portion corresponding to the central gas supply cell **62**, while the peripheral showerhead is defined by gas through-holes **56***a* at the electrode peripheral portion corresponding to the peripheral gas supply cell **64**. Further, flow rates per unit area may be set different, for the process gas delivered from the central showerhead and peripheral showerhead. Furthermore, gas types or gas mixture ratios are independently or respectively selected, for the process gas delivered from the central showerhead and peripheral showerhead.

[**0074**] The electrode support **58** of the inner upper electrode **38** is electrically connected to the first RF power supply **52** through the matching unit **44**, upper feed rod **46**, connector **48**, and lower feed cylinder **76**. The lower feed cylinder **76** is provided with a variable capacitor **78** disposed thereon, for variable adjusting capacitance.

[**0075**] Although not shown, the outer upper electrode **36** and inner upper electrode **38** may be provided with a suitable cooling medium space or cooling jacket (not shown) formed therein. A cooling medium is supplied into this cooling medium space or cooling jacket from an external chiller unit to control the electrode temperature.

[**0076**] An exhaust port **80** is formed at the bottom of the chamber **10**, and is connected to an exhaust unit **84** through an exhaust line **82**. The exhaust unit **84** includes a vacuum pump, such as a turbo molecular pump, to reduce the pressure of the plasma process space within the chamber **10** to a predetermined vacuum level. A transfer port for a semiconductor wafer W is formed in the sidewall of the chamber **10**, and is opened/closed by a gate valve **86** attached thereon.

[**0077**] In the plasma etching apparatus according to this embodiment, the susceptor **16** used as a lower electrode is electrically connected to a second RF power supply **90** through a matching unit **88**. The second RF power supply **90** outputs an RF voltage with a frequency of from 2 to 27 MHz, such as 2 MHz. The matching unit **88** is arranged to match the load impedance with the internal (or output) impedance of the RF power supply **90**. When plasma is generated within the chamber **10**, the matching unit **88** performs control for the load impedance and the internal impedance of the RF power supply **90** to apparently agree with each other.

[**0078**] The inner upper electrode **38** is electrically connected to a low-pass filter (LPF) **92**, which prevents the RF (60 MHz) from the first RF power supply **52** from passing through, while it allows the RF (2 MHz) from the second RF power supply **98** to pass through to ground. The low-pass filter (LPF) **92** is preferably formed of an LR filter or LC filter. Alternatively, only a single conductive line may be used for this, because it can give a sufficiently large reactance to the RF (60 MHz) from the first RF power supply **52**. On the other hand, the susceptor **16** is electrically connected to a high pass filter (HPF) **94**, which allows the RF (60 MHz) from the first RF power supply **52** to pass through to ground.

[**0079**] When etching is performed in the plasma etching apparatus, the gate valve **86** is first opened, and a semiconductor wafer W to be processed is transferred into the chamber **10** and placed on the susceptor **16**. Then, an etching gas (typically a mixture gas) is supplied from the process gas supply source **66** into the gas supply cells **62** and **64** at predetermined flow rates and flow-rate ratio. At the same time, the exhaust unit **84** is used to control the pressure inside the chamber **10**, i.e., the etching pressure, to be a predetermined value (for example, within a range of from several mTorr to 1 Torr). Further, a plasma generation RF (60 MHz) is applied from the first RF power supply **52** to the upper electrode **34** (**36** and **38**) at a predetermined power, while an RF (2 MHz) is applied from the second RF power supply **90** to the susceptor **16** at a predetermined power. Furthermore, a DC voltage is applied from the DC power supply **22** to the electrode **20** of the electrostatic chuck **18** to fix the semiconductor wafer W on the susceptor **16**. The etching gas delivered from the gas through-holes **56***a* of the inner upper electrode **38** is turned into plasma by glow discharge between the upper electrode **34** (**36** and **38**) and susceptor **16**. Radicals and ions generated in this plasma are used to etch the target surface of the semiconductor wafer W.

[**0080**] In this plasma etching apparatus, the upper electrode **34** is supplied with an RF within a range covering higher frequencies (form 5 to 10 MHz or more at which ions cannot follow). As a consequence, the plasma density is increased with a preferable dissociation state, so that high density plasma is formed even under a low pressure condition.

[**0081**] In the upper electrode **34**, the inner upper electrode **38** is also used as a showerhead directly across the semi-

conductor wafer W, such that the flow-rate ratio of the gas delivered from the central showerhead (**62** and **56***a*) and peripheral showerhead (**64** and **56***a*) can be arbitrarily adjusted. As a consequence, the spatial distribution of gas molecular or radical density can be controlled in the radial direction, so as to arbitrarily control the spatial distribution of an etching characteristic on the basis of radicals.

[**0082**] Further, as described later, the upper electrode **34** is operated as an RF electrode for plasma generation, such that the outer upper electrode **36** mainly works for it, and the inner upper electrode **38** assists it. The ratio of electric field intensity applied to electrons below the RF electrodes **36** and **38** can be adjusted by these electrodes. As a consequence, the spatial distribution of plasma density can be controlled in the radial direction, so as to arbitrarily and finely control the spatial distribution of a reactive ion etching characteristic.

[**0083**] It should be noted here that the control over the spatial distribution of plasma density has substantially no influence on the control over the spatial distribution of radical density. The control over the spatial distribution of plasma density is performed by varying the ratio of electric field intensity or input power between the outer upper electrode **36** and inner upper electrode **38**. On the other hand, the control over the spatial distribution of radical density is performed by varying the ratio of process gas flow rate, gas density, or gas mixture between the central showerhead (**62** and **56***a*) and peripheral showerhead (**64** and **56***a*).

[**0084**] The process gas delivered from the central showerhead (**62** and **56***a*) and peripheral showerhead (**64** and **56***a*) is dissociated in an area directly below the inner upper electrode **38**. Accordingly, even if the balance of electric field intensity between the inner upper electrode **38** and outer upper electrode **36** is changed, it does not have a large influence on the balance of radical generation amount or density between the central showerhead (**62** and **56***a*) and peripheral showerhead (**64** and **56***a*), because both showerheads belong to the inner upper electrode **38** (within the same area). Thus, the spatial distribution of plasma density and the spatial distribution of radical density can be controlled substantially independently of each other.

[**0085**] Further, the plasma etching apparatus is arranged such that most or the majority of plasma is generated directly below the outer upper electrode **36**, and then diffuses to the position directly below the inner upper electrode **38**. According to this arrangement, the showerhead or inner upper electrode **38** is less attacked by ions from the plasma. This effectively prevents the gas delivery ports **56***a* of the electrode plate **56** from being progressively sputtered, thereby remarkably prolonging the service life of the electrode plate **56**, which is a replacement part. On the other hand, the outer upper electrode **36** has no gas delivery ports at which electric field concentration occurs. As a consequence, the outer upper electrode **36** is less attacked by ions, and thus there arises no such a problem in that the outer upper electrode **36** shortens the service life in place of the inner upper electrode **38**.

[**0086**] As described above, **FIG. 2** shows a main part of the plasma etching apparatus (particularly, a main part of plasma generating means). In **FIG. 2**, the structure of the showerheads (**56***a*, **62**, and **64**) of the inner upper electrode **38** is not shown. **FIG. 3** is a circuit diagram showing an equivalent circuit of a main part of plasma generating means according to the first embodiment. In this equivalent circuit, the resistance of respective portions is not shown.

[**0087**] In this embodiment, as described above, the load circuit extending from the connector **48** comprises a coaxial path formed of the outer upper electrode **36** and feed cylinder **50** and the cylindrical grounded conductive body **10***a*, wherein the former members (**36** and **50**) function as a waveguide J_0. Where the radius (outer radius) of the feed cylinder **50** is a_0, and the radius of the cylindrical grounded conductive body **10***a* is b, the characteristic impedance or inductance L_0 of this coaxial path is approximated by the following formula (1).

$$L_0=K\times In(b/a_0) \quad (1)$$

[**0088**] In this formula, K is a constant determined by the mobility and dielectric constant of a conductive path.

[**0089**] On the other hand, the load circuit extending from the connector **48** also comprises a coaxial path formed of the lower feed rod **76** and the cylindrical grounded conductive body **10***a*, wherein the former member (**76**) functions as a waveguide J_i. Although the inner upper electrode **38** is present on the extension of the lower feed rod **76**, the impedance of lower feed rod **76** is dominant, because the difference in diameters between them is very large. Where the radius (outer radius) of the lower feed rod **76** is a_i, the characteristic impedance or inductance L_i of this coaxial path is approximated by the following formula (2).

$$L_i=K\times In(b/a_i) \quad (2)$$

[**0090**] As could be understood from the above formulas (1) and (2), the inner waveguide J_i for transmitting RF to the inner upper electrode **38** provides an inductance L_i in the same manner as a conventional ordinary RF system. On the other hand, the outer waveguide J_0 for transmitting RF to the outer upper electrode **36** provides a very small inductance L_0 because of a very large radius. As a consequence, in the load circuit extending from the connector **48** toward the side opposite to the matching unit **44**, RF is transmitted more easily through the outer waveguide J_0 having a lower impedance (a smaller voltage drop). The outer upper electrode **36** is thereby supplied with a larger RF power P_0, so the electric field intensity E_0 obtained at the bottom surface (plasma contact surface) of the outer upper electrode **36** becomes higher. On the other hand, RF is transmitted less easily through the inner waveguide J_i having a higher impedance (a larger voltage drop). The inner upper electrode **38** is thus supplied with an RF power P_i smaller than the RF power P_0 supplied to the inner upper electrode **38**, so the electric field intensity E_i obtained at the bottom surface (plasma contact surface) of the inner upper electrode **38** becomes lower than the electric field intensity E_0 on the outer upper electrode **36** side.

[**0091**] As described above, according to this upper electrode **34**, electrons are accelerated by a stronger electric field E_0 directly below the outer upper electrode **36**, while electrons are accelerated by a weaker electric field E_0 directly below the inner upper electrode **38**. In this case, most or the majority of plasma P is generated directly below the outer upper electrode **36**, while a subsidiary part of the plasma P is generated directly below the inner upper electrode **38**. Then, the high density plasma generated directly below the

outer upper electrode **36** diffuses radially inward and outward, so the plasma density becomes more uniform in the radial direction within the plasma process space between the upper electrode **34** and susceptor **16**.

[**0092**] Incidentally, in the coaxial path formed of the outer upper electrode **36** and feed cylinder **50** and the cylindrical grounded conductive body **10***a*, the maximum transmission power Pmax depends on the radius a_0 of the feed cylinder **50** and the radius b of the cylindrical grounded conductive body **10***a*, and is given by the following formula (3).

$$P\max/E_0^2 \max = a_0^2 [In(b/a_0)]^2/2Z_0 \quad (3)$$

[**0093**] In the above formula, Z_0 is the input impedance of this coaxial path viewing from the matching unit **44**, and E_0max is the maximum electric field intensity of the RF transmission system.

[**0094**] In the formula (3), the maximum transmission power Pmax takes on the maximum value when $(b/a_0) \approx 1.65$. In other words, when the ratio (b/a_0) of the radius of the cylindrical grounded conductive body **10***a* relative to the radius of the feed cylinder **50** is about 1.65, the power transmission efficiency of the outer waveguide J_0 is best. Accordingly, in order to improve the power transmission efficiency of the outer waveguide J_0, the radius of the feed cylinder **50** and/or the radius of the cylindrical grounded conductive body **10***a* are selected so that the ratio (b/a_0) is preferably set to be at least within a range of from 1.2 to 2.0, and more preferably within a range of from 1.5 to 1.7.

[**0095**] According to this embodiment, the lower feed rod **76** is provided with the variable capacitor **78** disposed thereon as means for adjusting the ratio or balance between the outer electric field intensity E_0 directly below the outer upper electrode **36** (or the input power P_0 into the outer upper electrode **36** side) and the inner electric field intensity E_i directly below the inner upper electrode **38** (or the input power P_i into the inner upper electrode **38** side), in order to arbitrarily and finely control the spatial distribution of plasma density. The capacitance C_{78} of the variable capacitor **78** is adjusted to increase or decrease the impedance or reactance of the inner waveguide J_i, thereby changing the relative ratio between the voltage drop through the outer waveguide J_0 and the voltage drop through the inner waveguide J_i. As a consequence, it is possible to adjust the ratio between the outer electric field intensity E_0 (outer input power P_0) and the inner electric field intensity E_i (inner input power P_i).

[**0096**] In general, the ion sheath impedance that causes an electric potential drop of plasma is capacitive. In the equivalent circuit shown in **FIG. 3**, it is assumed (constructed) that the sheath impedance capacitance directly below the outer upper electrode **36** is C_{po}, and the sheath impedance capacitance directly below the inner upper electrode **38** is C_{pi}. Further, the capacitance C_{40} of the capacitor formed between the outer upper electrode **36** and inner upper electrode **38** cooperates with the capacitance C_{78} of the variable capacitor **78** in changing the balance between the outer electric field intensity E_0 (outer input power P_0) and inner electric field intensity E_i (inner input power P_i). The capacitance C_{40} can be set or adjusted to optimize the variable capacitor's **78** function of adjusting the balance of electric field intensity (input power).

[**0097**] **FIGS. 4 and 5** show test examples (simulation data) in relation to the variable capacitor's **78** function of adjusting the balance of electric field intensity according to this embodiment. **FIG. 4** shows distribution characteristics of electric field intensity (relative value) in the radial direction of the electrode, using the capacitance C_{78} of the variable capacitor **78** as a parameter. **FIG. 5** shows the relative ratio between the outer electric field intensity E_0 and inner electric field intensity E_i, using the capacitance C_{78} of the variable capacitor **78** as a parameter.

[**0098**] In this simulation, the diameter of the semiconductor wafer W was set at 200 mm, the radius of the inner upper electrode **38** (with a circular plate shape) at 100 mm, and the inner radius and outer radius of the outer upper electrode **36** (with a ring shape) at 101 mm and 141 mm, respectively. In this case, the area of the semiconductor wafer W was 314 cm^2, the area of the inner upper electrode **38** was 314 cm^2 the same as that of the wafer W, and the area of the outer upper electrode **36** was 304 cm^2 slightly smaller than that of the wafer W. Typically, on the face opposite the wafer W, the planar area of the outer upper electrode **36** is preferably set to be about ¼ times to about 1 times the planar area of the inner upper electrode **38**.

[**0099**] As shown in **FIG. 4**, the outer electric field intensity E_0 directly below the outer upper electrode **36** is higher than the inner electric field intensity E_i directly below the inner upper electrode **38**, and a large step of electric field intensity is thereby formed near the boundary between the electrodes **36** and **38**. Particularly, the outer electric field intensity E_0 directly below the outer upper electrode **36** is apt to take on the maximum value near the boundary abutting the inner upper electrode **38**, and gradually decrease radially outward therefrom. In this example, as shown in **FIG. 5**, where the capacitance C_{78} of the variable capacitor **78** is changed within a range of from 180 to 350 pF, the ratio E_i/E_0 between the electric field intensities E_i and E_0 can be continuously controlled within a range of from about 10 to 40%. Where C_{78} falls within a range of from 125 to 180 pF, the load circuit produces resonance and thereby becomes uncontrollable. In principle, within a stable domain, where the capacitance C_{78} of the variable capacitor **78** is increased, the reactance of the inner waveguide J_i decreases. As a consequence, the inner electric field intensity E_i directly below the inner upper electrode **38** is relatively increased, so that the ratio E_i/E_0 between the outer electric field intensity E_0 and inner electric field intensity E_i is set to be higher.

[**0100**] According to this embodiment, the reactance of the outer waveguide J_0 provided by the feed cylinder **50** can be very small, so the impedance reactance of the load circuit, viewing from the output terminal of the matching unit **44**, takes on a capacitive negative value. This means that there is no resonance point at which reactance causes polar inversion from an inductive positive value to a negative value, on the waveguide extending from the output terminal of the matching unit **44** to the capacitive ion sheath. Since no resonance point is formed, no resonance electric current is generated, thereby reducing the RF energy loss and ensuring stable control of the plasma density distribution.

[**0101**] **FIGS. 6A** (bias in the ON-state), **6**B (bias in the OFF-state), **7**A (in the X direction), and **7**B (in the Y direction) show examples (experimental data) concerning electron density distribution characteristics and etching rate distribution characteristics, obtained by the plasma etching apparatus according to this embodiment. In this experiment,

as in the electric field intensity distribution characteristics shown in **FIGS. 4 and 5**, the capacitance C_{78} of the variable capacitor **78** was used as a parameter. The electron density was measured at positions in the radial direction, using a plasma absorption probe (PAP). Further, a silicon oxide film disposed on a semiconductor wafer was etched, and the etching rate was measured at wafer positions in the radial direction. Also in this experiment, the radius of the inner upper electrode **38** was set at 100 mm, and the inner radius and outer radius of the outer upper electrode **36** (with a ring shape) at 101 mm and 141 mm, respectively. Principal etching conditions were as follows:

[**0102**] Wafer diameter=200 mm;

[**0103**] Pressure inside the chamber=15 mTorr;

[**0104**] Temperature (upper electrode/chamber sidewall/lower electrode)=60/50/20° C.;

[**0105**] Heat transmission gas (He gas) supply pressure (central portion/edge portion)=15/25 Torr;

[**0106**] Distance between the upper and lower electrodes=50 mm;

[**0107**] Process gas ($C_5F_8/Ar/O_2$) flow rate≈20/380/20 sccm; and

[**0108**] RF power (60 MHz/2 MHz)≈2200 W/1500 W (C_{78}=500 pF, 1000 pF), 1800 W (C_{78}=120 pF).

[**0109**] Referring to **FIGS. 6A and 6B**, the capacitance C_{78} of the variable capacitor **78** was set at 120 pF so that the ratio E_i/E_0 between the outer electric field intensity E_0 and inner electric field intensity E_i was set to be higher. In this case, the distribution characteristic of electron density or plasma density was formed such that the density took on the maximum value near the electrode center, and monotonously decreased radially outward therefrom. It is thought that, in this case, the plasma diffusion rate overcame the difference between the plasma generation rate directly below the outer upper electrode **36** or the main plasma generation section, and the plasma generation rate directly below the inner upper electrode **38** or sub plasma generation section. As a consequence, the plasma gathered to the central portion from all around, and the plasma density was thereby higher at the central portion than at the peripheral portion.

[**0110**] On the other hand, the capacitance C_{78} of the variable capacitor **78** was set at 1000 pF so that the ratio E_i/E_0 between the outer electric field intensity E_0 and inner electric field intensity E_i was set to be lower. In this case, the distribution characteristic of electron density was formed such that the density took on the maximum value on the outer side (near a position 140 mm distant from the center) of the wafer rather than the inner side in the radial direction, and became almost uniform on the inner side (0 to 100 mm) of the wafer. It is thought that, this was so because the plasma generation rate directly below the inner upper electrode **38** increased, and plasma diffusion radially outward was thereby enhanced. In any case, the spatial distribution characteristic of electron density or plasma density can be flexibly and finely controlled by finely adjusting the capacitance C_{78} of the variable capacitor **78** within a suitable range.

[**0111**] Further, the electron density at respective positions was higher to some extent in the case (**FIG. 6A**) with an RF bias (2 MHz) applied to the lower electrode **16**, as compared to the case (**FIG. 6B**) without any RF bias applied to the lower electrode **16**. However, their distribution patterns were almost the same.

[**0112**] Referring to the experimental data shown in **FIGS. 7A and 7B**, different patterns of the spatial distribution characteristic of etching rate were formed by adjusting the capacitance C_{78} of the variable capacitor **78**, in accordance with the spatial distribution characteristics of electron density shown in **FIGS. 6A and 6B**. Accordingly, the spatial distribution characteristic of etching rate on the wafer surface can be flexibly and finely controlled by finely adjusting the capacitance C_{78} of the variable capacitor **78** within a suitable range.

[**0113**] Further, in the plasma etching apparatus according to this embodiment, the flow-rate ratio of the gas delivered from the central portion and peripheral portion can be adjusted by the showerhead mechanism of the inner upper electrode **36**, as described above. This function allows the spatial distribution characteristic of etching rate to be controlled on the basis of radicals.

Second Embodiment

[**0114**] **FIG. 8** is a sectional side view showing a plasma etching apparatus according to a second embodiment of the present invention. In **FIG. 8**, the constituent elements having substantially the same arrangement and function as those of the apparatus according to the first embodiment (**FIG. 1**) are denoted by the same reference numerals.

[**0115**] One of the features of the second embodiment resides in that the feed cylinder **50** or transmission path for transmitting the RF from the RF power supply **52** to the outer upper electrode **36** is made of a cast metal. This cast metal is preferably a metal having a high conductivity and workability, such as aluminum. As one of the advantages, cast metals can realize a low cost, and thus reduce the cost for the member to 1/7 or less of that provided by a plate material. As another advantage, cast metals can be easily integrated, and thus can reduce the number of RF connection surfaces in the member, thereby reducing the RF loss.

[**0116**] Further, even where the feed cylinder **50** is made of a cast metal, the RF transmission efficiency is not lowered. Specifically, referring to the experimental data shown in **FIGS. 9A** (cast metal), **9**B (plate), **10**A (cast metal), and **10**B (plate), there was no substantial difference in etching rate between the case where the feed cylinder **50** was made of a plate material, and the case where the feed cylinder **50** was made of a cast metal. **FIGS. 9A and 9B** show spatial distribution characteristics of etching rate over a silicon oxide film (SiO_2). **FIGS. 10A and 10B** show spatial distribution characteristics of etching rate over a photo-resist (PR) film. In this test example, principal etching conditions were as follows:

[**0117**] Wafer diameter=300 mm;

[**0118**] Pressure inside the chamber=25 mTorr;

[**0119**] Temperature (upper electrode/chamber sidewall/lower electrode)=60/60/20° C.;

[**0120**] Heat transmission gas (He gas) supply pressure (central portion/edge portion)=15/40 Torr;

[0121] Distance between the upper and lower electrodes=45 mm;

[0122] Process gas (C_5F_8/Ar/O_2) flow rate≈30/750/50 sccm;

[0123] RF power (60 MHz/2 MHz)≈3300 W/3800 W; and

[0124] Measurement time=120 seconds.

[0125] A second feature of the second embodiment resides in that a conductive ring member **100** is disposed around the feed rod **76** inside the feed cylinder **50**. The main role of the conductive member **100** is to reduce the inductance around the feed rod **76** so as to improve the range of the variable capacitor's **78** function of adjusting the balance between outer and inner input powers, as described below.

[0126] In this plasma processing apparatus, as described above, the ratio between the input power P_0 into the outer upper electrode **36** and the input power P_i into the inner upper electrode **38** can be arbitrarily adjusted by adjusting the capacitance C_{78} of the variable capacitor **78**. In general, the capacitance C_{78} of the variable capacitor **78** is adjusted stepwise, using a step motor or the like. For this capacitance adjustment, it is necessary to avoid the uncontrollable resonance domain described above (in **FIG. 5**, 125 pF<C_{78}<180 pF). For this reason, the experimental test examples described above according to the first embodiment (**FIGS. 6A, 6B**, 7A, and 7B) mainly used a stable domain (C_{78}≧= 180 pF) on the right side of the resonance domain. However, the stable domain on the right side has a limit in increasing the ratio of the inner input power P_i, and also entails a large power loss. On the other hand, as shown in **FIGS. 4 and 5**, a domain (C_{78}≦125 pF) on the left side of the resonance domain has an advantage in increasing the ratio of the inner input power P_i, as well as a smaller power loss. However, the domain on the left side of the resonance domain becomes closer to the resonance domain, as the ratio of the inner input power P_i is increased. In the case of a characteristic line with a large change rate (inclination), such as a characteristic line A shown in **FIG. 11**, it becomes very difficult to perform fine adjustment immediately before the resonance domain.

[0127] In order to solve this problem, it is effective to modify the characteristic line of capacitance vs. inner input power ratio, as indicated with a characteristic line B shown in **FIG. 11**, i.e., the change rate (inclination) in the domain on the left side of the resonance domain is set smaller so as to expand the adjusting range. Then, in order to obtain a characteristic line with a gentle and broader inclination as indicated with the characteristic line B shown in **FIG. 11**, it is effective to reduce the inductance L_i around the feed rod **76**, as described below.

[0128] **FIG. 12** is a circuit diagram showing an equivalent circuit of a plasma generation RF feed circuit according to the second embodiment. The reactance ωL_i around the feed rod **76** always takes on an absolute value larger than the reactance $1/\omega C_{78}$ of the capacitor **78**, and thus the composite reactance X of the inner waveguide J_i is always inductive and can be expressed by $X=\omega L_a$. A parallel circuit formed of this apparent inductance L_a and the capacitance C_{40} falls in a resonance state, when the susceptance $1/\omega L_a$ of the inductance L_a and the susceptance ωC_{40} of the capacitance C_{40} cancel each other to be zero, i.e., when $1/\omega L_a=1/(\omega L_i-1/\omega C_{78})=\omega C_{40}$ is satisfied. In this formula, with decrease in L_i, the value of C_{78} to establish the resonance condition described above increases, thereby approaching a characteristic line with a gentle and broader inclination immediately before the resonance domain, as indicated with the characteristic line B shown in **FIG. 11**. In the equivalent circuit shown in **FIG. 12**, the inductance L_0 of the outer waveguide J_0 is not shown, for the sake of simplicity of explanation. Even if the inductance L_0 is included in this equivalent circuit, the principle is the same.

[0129] **FIG. 13** shows an effect of the conductive member **100** according to this embodiment. When an electric current I varying with time flows through the feed rod **76**, a loop magnetic flux B is generated around the feed rod **76**, and an inductive electric current i interlinked with the magnetic flux B flows through the conductive member **100** due to electromagnetic induction. As a consequence, a loop magnetic flux b is generated inside and outside the conductive member **100** by the inductive electric current i, and the magnetic flux B is cancelled by that much corresponding to the magnetic flux b inside the conductive member **100**. Thus, the conductive member **100** disposed around the feed rod **76** can reduce the net magnetic flux generation amount around the feed rod **76**, thereby reducing the inductance L_i.

[0130] As regards the appearance structure of the conductive member **100**, a single ring shape continuous in an annular direction is preferably used, but a plurality of conductive members disposed in an annular direction may be used instead. As regards the inner structure of the conductive member **100**, a hollow ring body with a cavity shown in **FIG. 13** may be used, but a solid block structure, as shown in **FIG. 8**, can provide a large inductance reduction effect. The volume of the conductive member **100** is preferably set larger, and is ideally or most preferably set to fill the space inside the feed cylinder **50**. In practice, however, it is preferable for the conductive member **100** to occupy 1/10 to 1/3 of the space surrounded by the feed cylinder **50** and outer upper electrode **36**. The conductive member **100** is made of an arbitrary conductor material, such as aluminum or a cast metal. The conductive member **100** is disposed while being electrically insulated from conductive bodies around it, such as the feed rod **76** and inner upper electrode **38**.

[0131] **FIG. 14** shows experimental data of demonstration examples, in relation to the broadening effect described above of the conductive member **100** according to this embodiment. Referring to **FIG. 14**, a characteristic line B' was obtained by the apparatus structure according to this embodiment, and a characteristic line A' was obtained by the apparatus structure with no conductive member **100**. These characteristic lines A' and B' have upside-down shapes of the characteristic lines A and B shown in **FIG. 11**, respectively. Specifically, in a parallel-plate plasma apparatus of this type, as the ratio of the input power (inner input power P_i) into the central portion of the upper electrode **34** is increased, the plasma density becomes higher near the substrate W on the susceptor **16**, and the bias frequency Vpp on the susceptor **16** (in inverse proportion to the plasma density) decreases. According to this relationship, measurement values of Vpp obtained by respective step values of the variable capacitor **78** (a control variable in proportion to the value of the capacitance C_{78}) were plotted to obtain the characteristic lines A' and B', which thus have upside-down shapes of the characteristic lines A and B shown in **FIG. 11**, respectively.

According to this embodiment, thanks to the conductive member **100** disposed around the feed rod **76**, when the balance between the outer and inner input powers is adjusted by the variable capacitor **78**, the ratio of inner input power P_i can be stably and finely controlled to a value as high as possible immediately before the resonance domain, as demonstrated by the characteristic line B' shown in **FIG. 14**.

[**0132**] A third feature of the second embodiment relates to a low-pass filter **92** connected between the inner upper electrode **38** and ground potential. As shown in **FIG. 15A**, the low-pass filter **92** according to this embodiment is formed of a variable resistor **93** and a coil **95** connected in series, and arranged not to allow the plasma generation RF (60 MHz) to pass through, but to allow an alternating frequency of the bias RF (2 MHz) or less and DC to pass through. According to the low-pass filter **92**, the DC potential or self-bias voltage Vdc on the inner upper electrode **38** can be adjusted by adjusting the resistance value R**93** of variable resistor **93**.

[**0133**] More specifically, as shown in **FIG. 16**, as the resistance value R**93** of the resistor **93** is set lower, the voltage drop through the resistor **93** decreases, and the negative DC potential Vdc thereby becomes higher (closer to ground potential). Conversely, as the resistance value R**93** of the resistor **93** is set higher, the voltage drop through the resistor **93** increases, and the DC potential Vdc becomes lower. If the DC potential Vdc is too high (in general, it is higher than −150V), the plasma potential increases, thereby causing abnormal discharge or arcing. On the other hand, if the DC potential Vdc is too low (in general, it is lower than −450V), the inner upper electrode **38** is intensely attacked by ions, thereby hastening wear-out of the electrode.

[**0134**] In another perspective, as shown in **FIG. 17**, the DC potential Vdc has an appropriate range (from −450V to −150V) to prevent or suppress both of abnormal discharge and electrode wear-out, and the resistance value R**93** has a range (from Ra to Rb) corresponding to this appropriate range. Accordingly, the DC potential Vdc can be adjusted to be within the appropriate range described above (from −450V to −150V) by setting or adjusting the resistance value R**93** of the resistor **93** to be within the range described above (from Ra to Rb). Further, depending on the value of an RF power applied to the entire upper electrode **34** (outer upper electrode **36** and inner upper electrode **38**), the appropriate range (from Ra to Rb) of the resistance value R**93** changes. For example, in one experiment, the lower limit resistance value Ra=about 1 MΩ was provided by an RF power of 3000 W.

[**0135**] Further, as shown in **FIG. 15B**, the inner upper electrode **38** may be connected to ground through a variable DC power supply **97** to directly control the DC potential Vdc by the voltage of the power supply. The variable DC power supply **97** is preferably formed of a bipolar power supply.

[**0136**] A fourth feature of the second embodiment resides in that, in the upper electrode **34**, the bottom surface of the outer upper electrode **36** is protruded downward, i.e., toward the susceptor **16**, more than the bottom surface of the inner upper electrode **38**. **FIG. 18** is a sectional side view showing a main part of the plasma etching apparatus according to the second embodiment. In this example, the outer upper electrode **36** is formed of two parts divided in the vertical direction, i.e., an upper first electrode member **36**A and a lower second electrode member **36**B. The main body or first electrode member **36**A is made of, e.g., alumite-processed aluminum, and is connected to the feed cylinder **50**. The replacement part or second electrode member **36**B is made of, e.g., silicon, and is detachably fixed to and in close contact with the first electrode member **36**A by bolts (not shown). The second electrode member **36**B is protruded by a predetermined value H, relative to the bottom surface of the inner upper electrode **38**. A member **102** for enhancing thermal conductance, such as a silicone rubber sheet, is interposed between two electrode members **36**A and **36**B. The contact surfaces of the two electrode members **36**A and **36**B may be coated with Teflon™ to reduce thermal resistance.

[**0137**] In the outer upper electrode **36**, the protruded length H and inner diameter Φ of the protrusion part **36**B can define the intensity or direction of an electric field provided from the outer upper electrode **36** or upper electrode **34** to the plasma generation space. Thus, they are important factors to thereby determine the spatial distribution characteristic of plasma density.

[**0138**] **FIGS. 19A** to **19**E show examples (experimental data) concerning spatial distribution characteristics of electron density, using as parameters the protruded length H and inner diameter Φ of the protrusion part **36**B. Also in this experiment, the electron density was measured at positions in the radial direction, using a plasma absorption probe (PAP). The diameter of a semiconductor wafer was set at 300 mm. As regards the main parameters Φ and H, the experimental examples shown in **FIG. 19A** employed Φ=329 mm and H=15 mm, the experimental examples shown in **FIG. 19B** employed Φ=329 mm and H=20 mm, the experimental examples shown in **FIG. 19C** employed Φ=339 mm and H=20 mm, the experimental examples shown in **FIG. 19D** employed Φ=349 mm and H=20 mm, and the experimental examples shown in **FIG. 19E** employed Φ=359 mm and H=25 mm. As a secondary parameter, the ratio P_i/P_0 (RF power ratio) between the inner input power P_i and outer input power P_0 was set at four different values, i.e., (30/70), (27/73), (20/80), and (14/86).

[**0139**] In the experimental data shown in **FIGS. 19A** to **19**E, an inflection point F at which the electron density quickly drops was moved radially outward with increase in the inner diameter Φ of the protrusion part **36**B of the outer upper electrode **36**, and was moved up with increase in the protruded length H of the protrusion part **36**B. The ideal distribution characteristic is a characteristic in which an inflection point F is located directly above the wafer edge (a position of 150 mm), and the density is flat at a high value between the center and edge. In light of this, one characteristic (Φ=349 mm and H=20 mm) shown in **FIG. 19D** obtained by an RF power ratio P_i/P_0 of 30/70 is closest to the ideal state.

[**0140**] **FIG. 20A** shows characteristics of total uniformity U_T and edge uniformity U_E in the spatial distribution of electron density, using Φ and H as two-dimensional parameters. The total uniformity U_T stands for planar uniformity over the entire region in the radial direction from the wafer central position (R_0) to the wafer edge position (R_{150}), as shown in **FIG. 20B**. The edge uniformity U_E stands for planar uniformity over a region near the wafer edge, such as a region from a position of radius 130 mm (R_{130}) to the wafer edge position (R_{150}).

[0141] As understood from the characteristics shown in **FIG. 20A**, the protruded length H of the protrusion part **36**B is remarkably influential on the total uniformity U_T, and also has a large effect on the edge uniformity U_E. On the other hand, the inner diameter Φ of the protrusion part **36**B is influential on the edge uniformity U_E, but is scarcely influential on the total uniformity U_T. In total, the protruded length H of the protrusion part **36**B is preferably set at 25 mm or less, and most preferably set to be near 20 mm. The inner diameter Φ of the protrusion part **36**B is preferably set to be within a range of from 348 mm to 360 mm, and most preferably set to be near 349 mm. The range of from 348 mm to 360 mm means that the protrusion part **36**B is disposed at a position 24 mm to 30 mm distant from the wafer edge radially outward.

[0142] It should be noted that the protrusion part **36**B of the outer upper electrode **36** applies an electric field to the plasma generation space radially inward from around, thereby providing an effect of confining plasma. For this reason, the protrusion part **36**B is disposed preferably or almost essentially at a position outside the wafer edge in the radial direction, in order to improve uniformity in the spatial distribution characteristic of plasma density. On the other hand, the width of the protrusion part **36**B in the radial direction is not important, and thus can be arbitrarily set.

Third Embodiment

[0143] **FIG. 21** is a sectional side view showing a main part of a plasma etching apparatus according to a third embodiment of the present invention. The parts of this apparatus can be the same as those of the second embodiment except for the featuring parts. The third embodiment has a feature in that a shield member **104** is disposed along the protrusion part **36**B of the outer upper electrode **36** according to the second embodiment.

[0144] For example, the shield member **104** is formed of an aluminum plate with an alumite-processed surface, and physically and electrically coupled to the sidewall of the process container **10**. The shield member **104** extends essentially in the horizontal direction from the container sidewall to the position below the protrusion part **36**B of the outer upper electrode **36** to cover the bottom surfaces of the protrusion part **36**B and the ring-shaped shield member **42** in a non-contacting or insulated state. The second electrode member **36**B of the outer upper electrode **36** has an L-shaped cross section with a peripheral portion extending downward in the vertical direction to form a protrusion. The protruded length H and inner diameter Φ of this protrusion can be defined in accordance with the same numerical conditions as those of the second embodiment.

[0145] A function of the shield member **104** is to shield or seal RF discharge from the bottom surfaces of the protrusion part **36**B of the outer upper electrode **36** and ring-shaped shield member **42**, so as to suppress plasma generation directly below them. As a consequence, it is possible to primarily enhance the plasma confining effect directly above the wafer.

[0146] **FIGS. 22A** (with the shield member) and **22**B (without the shield member) show experimental data concerning the plasma confining effect provided by the shield member **104**. Where the shield member **104** was not used, as shown in **FIG. 22B**, the plasma electron density once dropped and then increased again to form a peak outside the wafer edge position (150 mm) in the radial direction. This was so because RF power was discharged vertically downward from the bottom surfaces of the protrusion part **36**B of the outer upper electrode **36** and ring-shaped shield member **42**, whereby plasma was also generated directly below them and thus electrons and ions were present there. Since a certain amount of plasma was present in a space distant from the wafer edge position radially outward, the plasma density directly above the wafer decreased by that much.

[0147] On the other hand, where the shield member **104** was used according to this embodiment, as shown in **FIG. 22A**, the electron density (plasma density) essentially monotonously decreased radially outward outside the wafer edge position (150 mm), while it was higher directly above the wafer as a whole. This was so because the bottom surfaces of the protrusion part **36**B of the outer upper electrode **36** and ring-shaped shield member **42** did not work as an RF path any more due to the presence of the shield member **104**, whereby plasma generation directly below them was remarkably reduced. The plasma confining effect or plasma diffusion-preventing effect of the shield member **104** was enhanced, with increase in the RF power of the RF power supply **52**.

[0148] Further, as a secondary effect, where plasma generation is remarkably reduced by the shield member **104** outside the wafer edge position, as described above, etching species, such as radicals and ions, are reduced. As a consequence, it is possible to effectively prevent undesirable polymer films from being deposited on portions inside the container (particularly near the shield member **104**).

[0149] For example, conventionally, where a Low-k film (an inter-level insulating film with a low dielectric constant) is etched, a plasma etching is performed, and then ashing (resist removal) is performed using O_2 gas within the same chamber. At this time, reactive species (such as CF and F), which have been deposited as polymers inside the container during the previous plasma etching, are activated by active oxygen atoms in plasma, and cause damage to the Low-k film (Low-k damages), such that they etch the via-holes of the film into a bowing shape or invade the film and change its k value. According to this embodiment, however, the shield member **104** can effectively prevent undesirable deposition of reactive species during plasma etching, thereby solving problems concerning Low-k damages described above. The shield member **104** may be made of an arbitrary conductor or semiconductor (such as, silicon), or a combination of different materials.

[0150] **FIG. 21** also shows an arrangement of cooling medium passages **106** and **108** formed in the upper electrode **34** (**36** and **38**). A cooling medium set at an adjusted temperature is circulated within each of the cooling medium passages **106** and **108** from a chiller unit (not shown) through lines **110** and **112**. Specifically, the cooling medium passages **106** are formed in the first electrode member **36**A of the outer upper electrode **36**. Since the second electrode member **36**B is coupled with the first electrode member **36**A through a coating or sheet **102** for enhancing thermal conductance, it can also be effectively cooled by the cooling mechanism.

[0151] The electrodes are supplied with a cooling medium even when the RF power supplies **52** and **90** are in the

OFF-state. Conventionally, the plasma processing apparatus of this type employs an insulative cooling medium, such as Galden™. In this case, when the cooling medium flows through a cooling medium passage, it generates an electrostatic charge by friction, by which the electrode enters an abnormally high voltage state. If an operator's hand touches the electrode in this state during a maintenance operation or the like in which the RF power supplies are in the OFF-state, the operator may get an electric shock. However, the plasma processing apparatus according to this embodiment allows electrostatic charge generated in the inner upper electrode **38** to be released to ground through the resistor **93** of the low-pass filter **92** (see **FIG. 8**), whereby an operator is prevented from getting an electric shock.

Fourth Embodiment

[**0152**] Using the plasma etching apparatus according to the third embodiment (**FIGS. 8 and 21**), an experiment was conducted of etching a silicon oxide film (SiO_2) to form a hole having a diameter (Φ) of 0.22 μm. In this experiment, etching characteristics (particularly etching rate) were examined, using as a parameter the RF power input ratio (P_i/P_0) between the outer upper electrode **36** and inner upper electrode **38**. Other etching conditions are shown below. FIGS. **23** to **25** show experimental result data.

[**0153**] Wafer diameter=300 mm;

[**0154**] Pressure inside the chamber=20 mTorr;

[**0155**] Temperature (upper electrode/chamber sidewall/lower electrode)=20/60/60° C.;

[**0156**] Heat transmission gas (He gas) supply pressure (central portion/edge portion)=20/35 Torr;

[**0157**] Distance between the upper and lower electrodes=45 mm;

[**0158**] Protruded length (H) of the outer upper electrode=15 mm;

[**0159**] Process gas ($C_5F_8/CH_2F_2/N_2/Ar/O_2$)≈10/20/110/560/10 sccm;

[**0160**] RF power (60 MHz/2 MHz)≈2300 W/3500 W; and

[**0161**] Etching time=120 seconds.

[**0162**] As shown in **FIG. 23**, as the ratio of the inner input power P_i increased, i.e., 14%, 18%, and 30%, the electron density or plasma density became higher in proportion to the P_i ratio near the wafer central portion, while it did not change near wafer edge portion. Accordingly, where the RF power input ratio (P_i/P_0) is adjusted on the basis of this, the spatial distribution characteristic of plasma density can be controlled in the radial direction.

[**0163**] **FIG. 24** shows the measurement result of deposition rate of a polymer film, formed from reaction products and reactive species, at respective positions in the radial direction, wherein the deposition rate is in proportion to radical density. This experiment was conducted to see the effect of change in the RF power input ratio (P_i/P_0) on the radical density. A bare silicon wafer was used as a sample substrate on which the polymer film was deposited. As indicated by the experimental data shown in **FIG. 24**, change in the RF power input ratio (P_i/P_0) only had a very small influence on the polymer film deposition rate i.e., the spatial distribution characteristic of radical density.

[**0164**] **FIG. 25** shows etching depth measured at respective positions of the wafer in the radial direction, obtained by the SiO_2 etching described above. As shown in **FIG. 25**, as the ratio of the inner input power P_i increased, i.e., 14%, 18%, and 30%, the etching depth became larger in proportion to the P_i ratio near the wafer central portion, while it did not differ so much near wafer edge portion. This was similar to that of the electron density (**FIG. 24**).

[**0165**] As described above, judging from the experimental data shown in FIGS. **23** to **25**, the following matters have been confirmed. Specifically, by adjusting the RF power input ratio (P_i/P_0) between the outer upper electrode **36** and inner upper electrode **38**, the spatial distribution characteristic of plasma density in the radial direction can be controlled without substantially affecting the spatial distribution characteristic of radical density, i.e., independently of the control over the spatial distribution of radical density. Accordingly, the uniformity of etching depth i.e., etching rate, can be improved by adjusting the RF power input ratio (P_i/P_0). It should be noted that, if the plasma etching apparatus according to the first or second embodiment (**FIGS. 1, 8**, and **18**) is used, the same experimental result as described above is obtained.

Fifth Embodiment

[**0166**] Using the plasma etching apparatus according to the third embodiment (**FIGS. 8 and 21**), a simulation was conducted of etching a silicon oxide film (SiO_2) with a CF family process gas. In this experiment, the distributions of radicals or reaction products were examined, using as a parameter the ratio (FC/FE) between the flow rate FC of a process gas delivered from the central showerhead (**62** and **56***a*) and the flow rate FE of the process gas delivered from the peripheral showerhead (**64** and **56***a*). In this simulation, it was assumed that neither reaction nor absorption of reaction products or reactive species was caused on the wafer surface, but the following reaction was simply caused on the blanket SiO_2 film.

$$2CF_2+SiO_2 \rightarrow SiF_4+2CO$$

[**0167**] Other principal etching conditions are shown below. FIGS. **26** to **30** show simulation result concerning radicals and reaction products. **FIG. 31** shows the type and generation rate (denoted by a percentage value in brackets) of radicals generated by gradual dissociation from molecules of the main etching gas (C_4F_8).

[**0168**] Wafer diameter=200 mm;

[**0169**] Pressure inside the chamber=50 mTorr;

[**0170**] Temperature (upper electrode/chamber sidewall/lower electrode)=20/60/60° C.;

[**0171**] Heat transmission gas (He gas) supply pressure (central portion/edge portion)=10/35 Torr;

[**0172**] Distance between the upper and lower electrodes=30 mm;

[**0173**] Protruded length (H) of the outer upper electrode=15 mm;

[0174] Process gas ($C_4F_8/N_2/Ar$)≈5/120/1000 sccm; and

[0175] RF power (60 MHz/2 MHz)≈1200 W/1700 W.

[0176] As shown in **FIG. 26**, the distribution characteristic of CF_2 density, which is the main reactive species, was remarkably influenced by the gas flow-rate ratio (FC/FE) between the center and periphery. Specifically, as the ratio of the central gas flow rate FC was increased, the CF_2 density became higher near the wafer central portion while it did not change so much near the wafer edge portion. As shown in **FIG. 28**, the distribution characteristic of CO radical density also showed a similar change with change in the gas flow-rate ratio (FC/FE) between the center and periphery. By contrast, as shown in **FIG. 27**, the distribution characteristic of Ar radical density scarcely changed with change in the gas flow-rate ratio (FC/FE) between the center and periphery.

[0177] As regards reaction products, as shown in **FIGS. 29 and 30**, either of SiF_4 density and CO density was remarkably influenced by the gas flow-rate ratio (FC/FE) between the center and periphery. More specifically, as the ratio of the central gas flow rate FC was reduced, each of the SiF_4 density and CO density became higher near the wafer central portion while it did not change so much near the wafer edge portion. Where the central gas flow rate FC was equal to the peripheral gas flow rate FE (FC/FE=50/50), the density became higher near the wafer central portion than near the wafer edge portion. As described above, reaction products tended to gather to the central side, because reaction products were less moved laterally by a fresh gas flow at the central portion, as compared with the peripheral portion.

[0178] If reaction products have a non-uniform distribution on a wafer, they not only affect the uniformity of process gas supply rate or chemical reaction among respective positions, but also may directly affect the etching shape or selectivity. According to this embodiment, as shown in **FIGS. 29 and 30**, where the central gas flow rate FC is set to be higher than the peripheral gas flow rate FE (FC/FE≈70/30 in this shown example), the space density distribution of reaction products can become uniform. It should be noted that, if the plasma etching apparatus according to the first or second embodiment (**FIGS. 1, 8**, and **18**) is used, the same simulation result as described above is obtained.

Sixth Embodiment

[0179] Using the plasma etching apparatus according to the third embodiment (**FIGS. 8 and 21**), an experiment was conducted of etching a BARC (antireflective film). In this experiment, the etching shape and selectivity were examined, using the gas flow-rate ratio (FC/FE) between the center and periphery as a parameter. A test sample shown in **FIG. 32A** was used. A mask having an opening diameter (Φ) of 0.12 μm, a photo-resist film having a thickness of 350 nm, a BARC film having a thickness of 80 nm, and an SiO_2 film having a thickness of 700 nm were used. "Oxide loss" and "resist remaining amount" were measured as examination items for the selectivity, and "bottom CD" was measured as an examination item for the etching shape or dimensional accuracy. **FIG. 32B** shows measurement values of the respective examination items at FC/FE=50/50. **FIG. 32C** shows measurement values of the respective examination items at FC/FE=70/30. As regards the measurement point, "center" denotes a position at the wafer center, and "edge" denotes a position 5 mm distant from the wafer notch end toward the center. Principal etching conditions were as follows:

[0180] Wafer diameter=300 mm;

[0181] Pressure inside the chamber=150 mTorr;

[0182] Heat transmission gas (He gas) supply pressure (central portion/edge portion)=10/25 Torr;

[0183] Distance between the upper and lower electrodes=30 mm;

[0184] Protruded length (H) of the outer upper electrode=15 mm;

[0185] Process gas (CF4)≈200 sccm;

[0186] RF power (60 MHz/2 MHz)≈500 W/600 W; and

[0187] Etching time=30 seconds.

[0188] As regards the examination items for the BARC etching, the "oxide loss" is the etched depth of the underlying SiO_2 film provided by over etching of the BARC etching. For this value, a smaller value is better, but a priority resides in that a smaller difference in this value over the wafer (particularly the difference between the center and edge) is better. The "resist remaining amount" is the thickness of the photo-resist remaining after the etching. For this value, a larger value is better, and a smaller difference in this value is also better. The "bottom CD" is the bottom diameter of a hole formed in the BARC. For this value, a value closer to the mask opening diameter Φ is better, and a smaller difference in this value is also better.

[0189] As shown in **FIG. 32B**, where the central gas flow rate FC was equal to the peripheral gas flow rate FE (5:5), the differences between the center and edge were large in all the examination items, and particularly the difference was large in the "resist remaining amount". By contrast, as shown in **FIG. 32B**, where the central gas flow rate FC was larger than the peripheral gas flow rate FE (7:3), all the examination items stably took on better values and became uniform between the center and edge, i.e., the selectivity and etching shape were remarkably improved.

[0190] As described above, according to this embodiment, within the process container **10**, particularly within the plasma generation space defined between the upper electrode **34** and lower electrode **16**, the inner upper electrode **38** of the upper electrode **34** is used while the ratio (FC/FE) between the process gas flow rate FC delivered from the central showerhead (**62** and **56***a*) and the process gas flow rate FE (**64** and **56***a*) delivered from the peripheral showerhead is adjusted. As a consequence, the spatial distribution of radical density can be controlled to uniformize etching characteristics (such as the selectivity and etching shape) on the basis of radicals. It should be noted that, if the plasma etching apparatus according to the first or second embodiment (**FIGS. 1, 8**, and **18**) is used, the same measurement result as described above is obtained.

Seventh Embodiment

[0191] Using the plasma etching apparatus according to the third embodiment (**FIGS. 8 and 21**), an experiment was conducted of etching an SiO_2 film. In this experiment, the

etching shape was examined, using the gas flow-rate ratio (FC/FE) between the center and periphery as a parameter. A test sample shown in **FIG. 33A** was used. A mask having an opening diameter (Φ) of 0.22 μm, a photo-resist film having a thickness of 500 nm, a BARC film having a thickness of 100 nm, and an SiO_2 film having a thickness of 1 μm were used. "Etching depth", "top CD", and "bottom CD" were measured as examination items for the etching shape. **FIG. 33B** shows measurement values of the respective examination items at FC/FE=50/50. **FIG. 33C** shows measurement values of the respective examination items at FC/FE=10/90. Principal etching conditions were as follows:

[**0192**] Wafer diameter=300 mm;

[**0193**] Pressure inside the chamber=20 mTorr;

[**0194**] Temperature (upper electrode/chamber sidewall/lower electrode)=20/60/60° C.

[**0195**] Heat transmission gas (He gas) supply pressure (central portion/edge portion)=20/35 Torr;

[**0196**] Distance between the upper and lower electrodes=45 mm;

[**0197**] Protruded length (H) of the outer upper electrode=15 mm;

[**0198**] Process gas ($C_5F_8/CH_2F_2/N_2/Ar/O_2$)≈10/20/110/560/10 sccm;

[**0199**] RF power (60 MHz/2 MHz)≈2300 W/3500 W;

[**0200**] RF power ratio (inner input power P_i/outer input power P_0)=30:70; and

[**0201**] Etching time=120 seconds.

[**0202**] As regards the examination items for the SiO_2 etching, the "etching depth" is the depth of a hole formed in the SiO_2 film by the etching time (120 seconds), i.e., it corresponds to the etching rate. The "top CD" and "bottom CD" are the top and bottom diameters of the hole formed in the SiO_2 film, and, as these values are closer to each other, the vertical shape characteristic of the hole (anisotropy) is better. As a matter of course, for each of the examination items, it is more preferable that the difference between the center and edge is smaller.

[**0203**] As shown in **FIG. 33B**, where the central gas flow rate FC was equal to the peripheral gas flow rate FE (5:5), the difference was large in the "etching depth", and values of the ratio of bottom CD/top CD at respective positions were small, i.e., the holes were more tapered. By contrast, as shown in **FIG. 33B**, where the central gas flow rate FC was smaller than the peripheral gas flow rate FE (1:9), the "etching depth" i.e., etching rate became more uniform, and the vertical shape characteristic was improved and more uniform.

[**0204**] As described above, also in this embodiment, by adjusting the ratio (FC/FE) between the inner gas flow rate FC and the outer gas flow rate FE, the spatial distribution of radical density can be controlled to uniformize etching characteristics (particularly the etching shape) on the basis of radicals. It should be noted that, if the plasma etching apparatus according to the first or second embodiment (**FIGS. 1, 8**, and **18**) is used, the same measurement result as described above is obtained.

[**0205**] According to the embodiments described above, the plasma density distribution and the radical density distribution can be controlled independently of each other within the plasma generation space defined in the process container **10**. This independent control over two systems can be used to preferably deal with various plasma process applications, such as those shown in the map of **FIG. 34**.

[**0206**] The embodiments described above may be modified in various manners, in accordance with the technical ideas of the present invention. For example, only the outer upper electrode **36** may be supplied with an RF from the first RF power supply **52** through the matching unit **44** and feed cylinder **50**, while the inner upper electrode **38** being supplied with no RF. Also in this case, the inner upper electrode **38** can function as a showerhead or function as an electrode for an RF output from the second RF power supply **90** to flow to ground. Alternatively, the inner upper electrode **38** may be replaced with a single-purpose showerhead with no electrode function. In the embodiments described above, the outer upper electrode **36** is formed of one or single ring electrode, but it may be formed of a plurality of electrodes combined to form a ring as a whole. Further, the inner diameter of the outer upper electrode **36** may be set very small, or the outer upper electrode **36** may be formed of a circular plate. Depending on the application, the second RF power supply **90** may be omitted. The present invention can be applied not only to plasma etching, but also to various plasma processes, such as plasma CVD, plasma oxidation, plasma nitridation, and sputtering. As regards a target substrate, the present invention can be applied not only to a semiconductor wafer, but also to various substrates for a flat panel display, photo mask, CD substrate, and print substrate.

[**0207**] Additional advantages and modifications will readily occur to those skilled in the art. Therefore, the invention in its broader aspects is not limited to the specific details and representative embodiments shown and described herein. Accordingly, various modifications may be made without departing from the spirit or scope of the general inventive concept as defined by the appended claims and their equivalents.

1. A plasma processing method comprising:

supplying a predetermined process gas into a plasma generation space in which a target substrate is placed, and turning the process gas into plasma; and

subjecting the substrate to a predetermined plasma process by the plasma,

wherein spatial distribution of density of the plasma and spatial distribution of density of radicals in the plasma relative to the substrate are controlled independently of each other by a set of first and second RF discharge regions and a set of first and second process gas delivery regions, respectively, to form a predetermined process state over an entire target surface of the substrate, and

wherein the set of first and second RF discharge regions and the set of first and second process gas delivery regions are disposed in layouts independently of each other.

2. The method according to claim 1, wherein a facing portion opposite the substrate is divided into two regions as the first and second RF discharge regions on a peripheral side and a central side, respectively, in a radial direction relative to a center through which a vertical line extending from a center of the substrate passes; and

the second RF discharge region on the facing portion is divided into two regions as the first and second process gas delivery regions on a peripheral side and a central side, respectively, in the radial direction.

3. The method according to claim 2, wherein the first RF discharge region is disposed radially outside an outer peripheral edge of the substrate.

4. The method according to claim 1, wherein an RF output from a single RF power supply is divided at a predetermined ratio, and thereby discharged from the first RF discharge region and the second RF discharge region.

5. The method according to claim 1, wherein a process gas supplied from a single process gas supply source is divided at a predetermined ratio, and thereby delivered from the first process gas delivery region and the second process gas delivery region.

6. The method according to claim 5, wherein the process gas is delivered from the first and second process gas delivery regions at deferent flow rates per unit area.

7. The method according to claim 1, wherein the process gas is a mixture gas of a plurality of gases, the plurality of gases are delivered from the first process gas delivery region at a first gas mixture ratio, and the plurality of gases are delivered from the second process gas delivery region at a second gas mixture ratio different from the first gas mixture ratio.

8. A plasma processing method comprising:

exposing a target substrate to plasma of a predetermined process gas; and

subjecting the substrate to a predetermined plasma process by the plasma,

wherein spatial distribution of density of the plasma and spatial distribution of density of radicals in the plasma are controlled independently of each other relative to the substrate to form a predetermined process state over an entire target surface of the substrate, and

wherein processing rates at respective positions on the target surface of the substrate are mainly controlled in accordance with the plasma density spatial distribution, and one or both of processing selectivity and processing shapes at respective positions on the target surface are mainly controlled in accordance with the radical density spatial distribution.

9. The method according to claim 1, wherein the first and second RF discharge regions comprise an RF electrode to be supplied with an RF.

10. A plasma processing apparatus arranged to turn a process gas into plasma in a plasma generation space within a process container configured to have a vacuum atmosphere therein, and subject a target substrate placed within the plasma generation space to a predetermined plasma process, the apparatus comprising:

a plasma density control section configured to control spatial distribution of density of the plasma relative to the substrate; and

a radical density control section configured to control spatial distribution of density of radicals in the plasma relative to the substrate independently of the plasma density spatial distribution,

wherein the plasma density control section comprises a set of first and second RF discharge regions configured to control the plasma density spatial distribution,

the radical density control section comprises a set of first and second process gas delivery regions configured to control the radical density spatial distribution, and

the set of first and second RF discharge regions and the set of first and second process gas delivery regions are disposed in layouts independently of each other.

11. The apparatus according to claim 10, wherein a facing portion opposite the substrate and in contact with the plasma generation space is divided into two regions as the first and second RF discharge regions on a peripheral side and a central side, respectively, in a radial direction relative to a center through which a vertical line extending from a center of the substrate passes; and

the second RF discharge region on the facing portion is divided into two regions as the first and second process gas delivery regions on a peripheral side and a central side, respectively, in the radial direction.

12. The apparatus according to claim 11, wherein the first RF discharge region is disposed radially outside an outer peripheral edge of the substrate.

13. The apparatus according to claim 10, wherein the process gas is a mixture gas of a plurality of gases, the plurality of gases are delivered from the first process gas delivery region at a first gas mixture ratio, and the plurality of gases are delivered from the second process gas delivery region at a second gas mixture ratio different from the first gas mixture ratio.

14. The apparatus according to claim 10, wherein an RF power is discharged toward the plasma space from the first and second RF discharge regions at a predetermined ratio; and

the process gas is delivered toward the plasma space from the first and second process gas delivery regions at a predetermined ratio.

15. The apparatus according to claim 14, wherein the plasma density control section comprises an RF distributor configured to divide and transmit an RF with a constant frequency, output from an RF power supply, at a predetermined ratio to the first and second RF discharge regions; and

the radical density control section comprises a process gas distributor configured to divide and supply the process gas, output from a process gas supply source, at a predetermined ratio to the first and second process gas delivery regions.

16. The apparatus according to claim 15, wherein the RF distributor includes an impedance control section configured to variably control one or both of an impedance of a first feed circuit from the RF power supply to the first RF discharge region, and an impedance of a second feed circuit from the RF power supply to the second RF discharge region.

17. The apparatus according to claim 10, wherein the first and second RF discharge regions respectively comprise first and second electrodes electrically insulated from each other.

18. The apparatus according to claim 17, wherein the first and second process gas delivery regions include a number of process gas delivery holes formed on the second electrode.

* * * * *